



## LJMU Research Online

Lynch, SFL, Batty, LC and Byrne, PA

**Environmental risk of severely Pb-contaminated riverbank sediment as a consequence of hydrometeorological perturbation**

<http://researchonline.ljmu.ac.uk/8605/>

### Article

**Citation** (please note it is advisable to refer to the publisher's version if you intend to cite from this work)

**Lynch, SFL, Batty, LC and Byrne, PA (2018) Environmental risk of severely Pb-contaminated riverbank sediment as a consequence of hydrometeorological perturbation. *Science of the Total Environment*, 636. pp. 1428-1441. ISSN 0048-9697**

LJMU has developed **LJMU Research Online** for users to access the research output of the University more effectively. Copyright © and Moral Rights for the papers on this site are retained by the individual authors and/or other copyright owners. Users may download and/or print one copy of any article(s) in LJMU Research Online to facilitate their private study or for non-commercial research. You may not engage in further distribution of the material or use it for any profit-making activities or any commercial gain.

The version presented here may differ from the published version or from the version of the record. Please see the repository URL above for details on accessing the published version and note that access may require a subscription.

For more information please contact [researchonline@ljmu.ac.uk](mailto:researchonline@ljmu.ac.uk)

<http://researchonline.ljmu.ac.uk/>



26           **1. Introduction**

27   Metal mining activities including mineral extraction, processing and dumping of contaminated waste  
28   alongside river channels has resulted in the widespread metal pollution of soils and sediments and is  
29   a worldwide health concern (Foulds et al 2014; Zhang et al 2012; Zadnik 2010). The impacts of these  
30   activities have been reported internationally; Coeur d'Alene River Valley, Idaho (USGS 2001), San  
31   Luis, Argentina (Tripole et al 2006) and throughout Europe, Upper Silesia in southern Poland (Ullrich  
32   et al. 1999), Iberian Pyrite Belt, south west Spain (Torres et al 2013). In England and Wales, mining  
33   impacted catchments play a critical role in the distribution of metals through fluvial systems with the  
34   highest metal flux arising from mineralised catchments with a history of metal mining (Mayes et al.  
35   2013). Contrary to the traditional focus on point sources of pollution from adits and shafts, a greater  
36   emphasis has been placed on dealing with diffuse forms, primarily due to the EU Water Framework  
37   Directive 2000/60/EC requirement that management of water quality should be at a catchment scale  
38   delivered through the river basin management plans (Collins et al. 2012). There are 226 waterbodies  
39   categorised as 'impacted' by non-coal mine water pollution in England and Wales and over 50% show  
40   evidence of diffuse pollution (Environment Agency 2010). That could serve as a barrier to achieving  
41   'good' surface water chemical status for all water bodies by 2021 (EU amending directives  
42   2000/60/EC and 2008/105/EC). Identifying the exact sources, and understanding pollution dynamics,  
43   within a catchment are listed as key priorities for effective management and remediation efforts  
44   (Environment Agency 2012a).

45   Pb is listed as a priority substance in EU amending directives 2000/60/EC and 2008/105/EC in the  
46   field of water policy because of its known toxic effects. Unlike elements, such as Cu and Zn, Pb has  
47   no known biological function and therefore can be harmful to flora and fauna at very low levels  
48   (Chibuikwe and Obiora 2014). Pb is bioaccumulative, passing through trophic levels of the food chain  
49   and increasing in concentration at each level. Bioavailable forms of Pb can be taken up and stored in  
50   tolerant plants (Sharma and Dubey 2005) and macroinvertebrates (Cid et al. 2010), accumulate in  
51   earthworms (Wijayawardena et al. 2017) and high concentrations can be stored in liver, kidneys and  
52   muscles of cattle due to the consumption of contaminated forage (Zadnik 2010). In severely  
53   contaminated mining catchments such as Coeur d'Alene river Basin, USA, levels of Pb in children's  
54   blood have been found to far exceed federal intervention levels (USGS 2001). Pb can have chronic

55 and acute toxicity effects that include detrimentally impacting macroinvertebrate community structure  
56 (Montserrat 2010; Byrne et al. 2013), phytotoxicity resulting in riverbank instability (Environment  
57 Agency 2008), chronic effects in cattle such as osteoporosis and anaemia with high exposure  
58 resulting in ataxia and death (Zadnik 2010) and neurotoxic effects in children such as behaviour  
59 problems, lower IQ and learning disabilities (Wijayawardena et al 2017).

60 In mining impacted catchments Pb can be introduced into the environment when primary sulphide  
61 mineral galena (PbS) is brought to the surface and oxidised through exposure to atmospheric  
62 conditions. High concentrations of Pb and sulphate can be released into fluvial systems in this way.  
63 Once introduced to the river system Pb can be transported downstream as a free ion, aqueous  
64 complex, or in particulate form sorbed to sediment particles (vanLoon and Duffy 2011). Where  
65 physical, chemical and hydrological changes within the river allow, Pb associated sediment would be  
66 deposited on riverbanks and floodplains, the location depending on factors such as particle size, flood  
67 magnitude and morphology of the river (Macklin and Dowsett 1989; Bradley 1995; Dennis et al.  
68 2003). The partitioning of Pb in sediment is dependent on the chemical environmental conditions and  
69 the geology, for example formations high in quartz or carbonates that would influence mineralogy.  
70 Where Pb is associated with mineral forms impervious to weathering, environmental changes would  
71 not influence the mobilisation of dissolved Pb and this contaminant would remain unavailable for  
72 uptake. However in mining impacted catchments Pb is often associated with Fe and Mn (hydr)oxide  
73 and sulphur minerals in the sediment (Tripole et al 2006; Buekers et al 2008; Zakir and Shikazono  
74 2011). These minerals can undergo dissolution and precipitation reactions in response to dynamic  
75 changes in redox potential, pH (Nordstrom and Alpers 1999) and levels of moisture (Buckby et al.  
76 2003) – processes that commonly occur within the riverbank environment (Byrne et al. 2013; Krause  
77 et al. 2010; Du Laing et al. 2009). As a result the sediment can become a source of dissolved Pb to  
78 river systems (Charlatchka and Cambier 2000; Torres et al 2013).

79 Climate projections based on UKCP09 river basin regions in West Wales and North West England  
80 (Met Office 2017) indicate a shift towards aridity by 2020. Summer river flows are expected to decline  
81 and Q95 (flow that is exceeded 95% of the time) may reduce 26% by 2050 and 35% by 2080 in  
82 western Wales, using medium emissions (P50) scenarios (DEFRA 2012a). Furthermore projections  
83 indicate a rise in the occurrence of localized heavy rainfall events, particularly in winter. Peak river

84 flows are expected to increase 13% by 2020, 20.8% by 2050 and 27.6% by 2080 in Wales, using  
85 medium (P50) scenarios (DEFRA 2012b). Changes in river flow alter river stage and expose river  
86 bank sediments to variable water saturation regimes, periods of inundation are followed by periods of  
87 drainage. If climate change projections are correct, patterns of inundation and drainage are likely to  
88 become more pronounced. The focus of the current research is within the UK, however it is important  
89 to note that climate driven changes in distribution of rainfall and the resulting increase in peak flow  
90 events within mining impacted systems, is an issue experienced internationally (Ciszewski and Grygar  
91 2016).

92 The current research is intended to add to the work of Lynch et al. (2017) in which the geochemical  
93 mechanisms controlling dissolved Zn release from riverbank sediments were determined (Lynch et al.  
94 2017). Key Zn control mechanisms were: The (co)precipitation of Zn with Mn (hydroxides), followed  
95 by the reductive dissolution and release of Zn in response to prolonged flooding and; Precipitation of  
96 Zn sulphate salts over long dry antecedent periods followed by the immediate dissolution of these  
97 salts and release of dissolved Zn on sediment flood wetting.

98 In the current study the same mesocosm experiments are run to allow the authors to determine the  
99 control that different sequential patterns of flooding and drainage have on the mobilisation of  
100 dissolved Pb. Pb is reported as less mobile than Zn under oxic conditions (Galan et al. 2003; Carroll  
101 et al. 1998) with a greater affinity for Fe (hydr)oxide surfaces (Evans 1991; Wang 2010) and a lower  
102 sorption edge (Lee et al 2002; Appelo and Postma 2010). However, in severely polluted catchments  
103 contaminated sediments have been identified as an important source of dissolved Pb contamination  
104 to surface water (Palumbo-Roe et al 2012; Byrne et al 2013) and it is hypothesised that certain  
105 flood/drain sequences will control the mobilisation of dissolved Pb from contaminated riverbank  
106 sediment.

107 Key hydrogeochemical mechanisms may include: (i) Pb co-precipitation with and sorption to Fe/Mn  
108 (hydr)oxides under oxidised (drained) periods followed by reductive dissolution and release of  
109 dissolved Pb due to a fall in redox potential conditions over prolonged flood periods; (ii) the oxidation  
110 of the primary mineral galena and release of dissolved Pb and sulphate where previously reduced  
111 sediment is exposed to oxic conditions (Wragg and Palumbo-Roe 2011) (iii) the precipitation of  
112 insoluble Pb sulphides due to a fall in redox potential conditions over prolonged flood periods (Lynch

113 et al 2014); (iv) control of dissolved Pb concentrations to low levels through saturation with respect to  
114 anglesite ( $\text{PbSO}_4$ ) over flooded periods (Palumbo-Roe et al. 2013; Appelo and Postma 2010); (v)  
115 hydrological saturation and precipitation of soluble sulphate salts over long dry periods followed by  
116 dissolution of these salts, and a 'flush' of dissolved Pb and sulphate, in response to flood wetting  
117 (Byrne et al. 2013).

118 Previous studies have investigated the effects of alternately flooding and drying contaminated soil for  
119 different frequencies and durations on the mobilisation of toxic trace elements such as Cd and Zn  
120 (Lynch et al 2017; Shaheen et al 2014; Du Laing et al 2007). This study is unique in that experiments  
121 examine the patterns of dissolved Pb release from coarse grained riverbank sediment collected from  
122 a mining impacted catchment highly contaminated with Pb. Understanding the mechanisms of release  
123 for this toxic metal under varying hydrometeorological perturbations is crucial information for  
124 environmental monitoring and the development of successful pollution control measures.

125 To establish the environmental risk Pb-contaminated riverbank sediment may pose in light of UK  
126 climate projections, the results of two laboratory mesocosm experiments are examined. The  
127 objectives were to: (i) Investigate if flooding and draining sequences influence the patterns of  
128 dissolved Pb release from severely contaminated river bank sediment; (ii) Identify key  
129 hydrogeochemical processes responsible for controlling the mobilisation of dissolved Pb and if they  
130 differ from the mechanisms of control for dissolved Zn; (iii) Establish if Pb contaminated riverbank  
131 sediment poses an environmental risk when exposed to alternate flooding and draining sequences;

## 132 **2. Introduction**

133 A summary of the sample site data and mesocosm treatment methods is provided below. Please see  
134 (Lynch et al. 2017) for detailed information on the methodology.

### 135 **2.1 Sediment sample site**

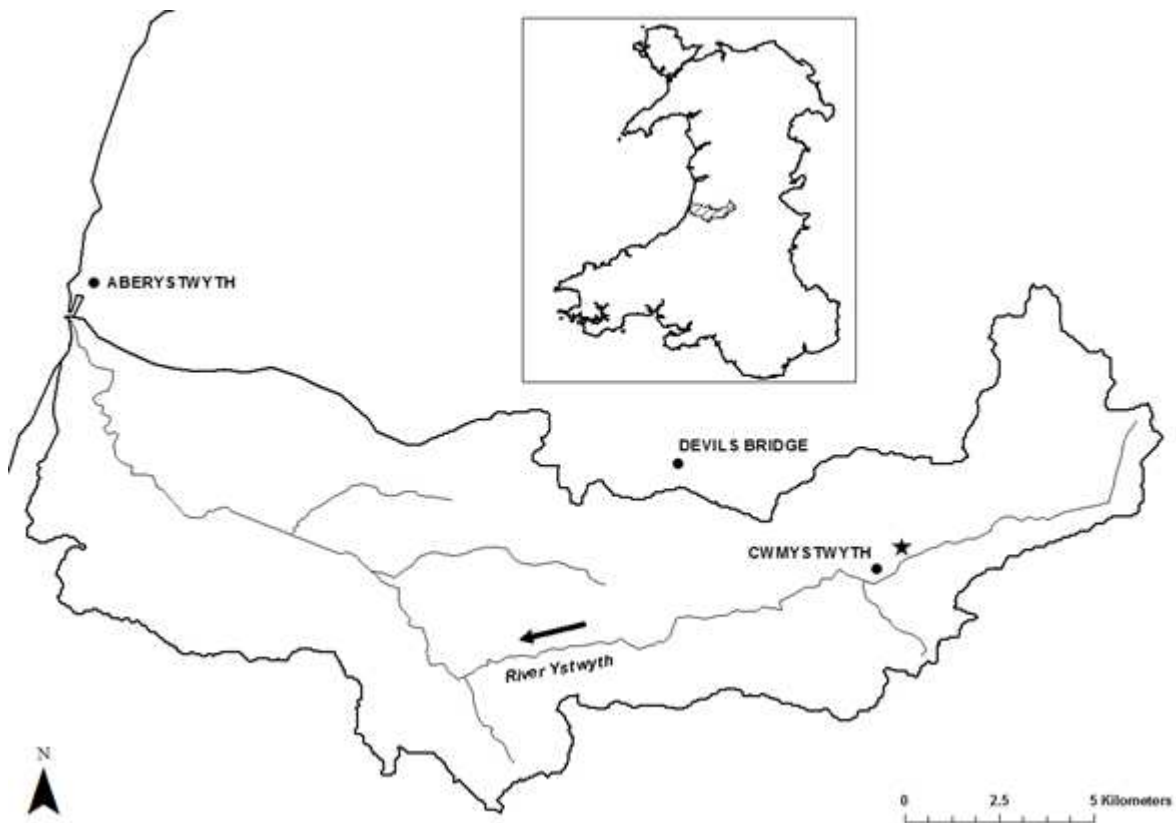
136 The sample site at Cwmystwyth (SN799743) is located in central Wales, at an elevation of 250 m above  
137 sea level (ASL). The mine site is drained by the Afon Ystwyth River which runs from east to west,  
138 draining into the Irish Sea at Aberystwyth (approximately 25 km north east of Cwmystwyth) (Fig1). The  
139 north side of the river is marked by spoil heaps rising to 500 m ASL and on the south side grass banks,  
140 used primarily for grazing, rise steeply to 450 m ASL. Mining ceased at Cwmystwyth in 1921 (Bick

141 1976). The country rock dates from the Silurian period with alternating bedrock of hard coarse  
142 sandstones and shales that form the upper Llandovery Series (British Geological Survey 2007). Rivers  
143 that rise on this type of geology have been described as 'Base Poor' having a low alkalinity, so less  
144 able to buffer acidic inputs (Natural Resources Wales 2004).

145

## 146 **2.2 Rainfall and river flow characteristics**

147 Detailed information on rainfall and flow at the sample site can be found in Lynch et al (2017). Generally  
148 flow rises and recedes quickly, however extended periods (greater than a week) of flow well above the  
149 mean value (1.989 m<sup>3</sup>/s) (leading to riverbank and floodplain inundation) and extended periods well  
150 below the mean value (leading to drainage and exposure of riverbank and floodplain), are common  
151 (Centre for Ecology and Hydrology 2015). Changes in river flow are known to cause a rise and fall in  
152 river stage that can influence patterns of hyporheic exchange flow (Byrne et al. 2013).



153

154

155 Fig. 1 Location of sample site, grid reference SN799743 (denoted by a star) at the Cwmystwyth  
156 abandoned mine complex in the River Ystwyth catchment in mid-Wales (inset)

157

## 158 **2.3 Sediment collection**

159 Sediment was collected on two occasions, July 2012 and December 2013 for analysis in two separate  
160 mesocosm treatments. Visual inspection of the northern riverbank indicated that sediment was made  
161 up of predominantly sandy gravel interspersed with some finer silt particles and larger pebbles and  
162 boulders. The sediment samples were collected from the north bank of the river at the same site, but  
163 different locations. On the first visit, sediment was taken from waste piles running along the side of the  
164 river channel. This material would have been dumped along the side of the river during active mining  
165 and was therefore likely to contain high concentrations of primary and secondary minerals. On the  
166 second visit, material was taken from the base of the mining waste piles, on a lateral flow path, so  
167 was likely to contain lower concentrations of the primary waste and material eroded from the waste  
168 piles. This site was closer to the active river channel and therefore would be more susceptible to  
169 hydrometeorological perturbations. A stainless steel shovel was used to collect sediment from the top  
170 10 cm.

## 171 **2.4 Laboratory analysis**

### 172 **2.4.1 Mesocosm experiments**

173 Two mesocosm experiments were conducted in order to meet the objectives. The first experiment was  
174 run to determine the effect alternately wetting and drying contaminated sediment for different durations  
175 and frequencies had on the release of dissolved Pb and establish whether the sediment posed an  
176 environmental risk. The second experiment focused on runs where patterns of dissolved Pb release  
177 were pronounced allowing a (i) comparison of concentration and lability of Pb in the sediment at the two  
178 different sampling locations; (ii) comparison of the environmental risk the sediment posed at each  
179 location (iii) determination of the repeatability of the results. For both experiments water and sediment  
180 analysis enabled the elucidation of the key geochemical mechanisms of dissolved Pb mobilisation.  
181 The sediment was homogenised by hand and larger pebbles were removed. The sediment was then  
182 packed into each mesocosm to a depth of 24 cm using a plastic trowel (Fig. 2). An extended  
183 experimental timeframe for each column of 20 days at field capacity, to equilibrate the sediment,  
184 followed by a maximum of 11 weeks treatment period promoted the removal of any artefacts and  
185 allowed time for systems to settle into a steady pattern. Artificial Rainwater (ARW) was created based  
186 on Plynlimon rainwater chemistry (pH 4.9 - 5.2), found in the uplands of mid-Wales (Neal et al. 2001).  
187 For field capacity, twice a week, 500 ml of ARW was added via the top of the mesocosm until water

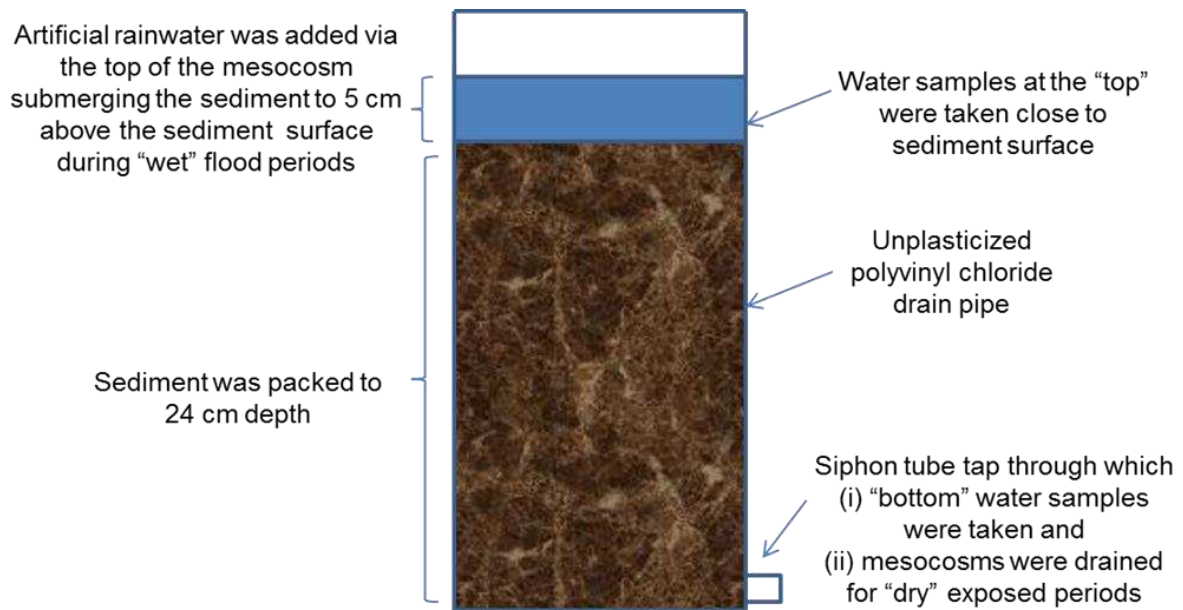


188 percolated through the bottom tap (Fig. 2). Following field capacity, mesocosms were divided into 7  
189 different treatments. 5 were variable wet and dry runs and 2 constant controls. The Cwmystwyth gauged  
190 daily flow (grid reference SN790737), taken from the UK National River Flow Archive (Centre for  
191 Ecology and Hydrology 2015), provided guidance regarding the length of time riverbank sediment may  
192 be exposed to atmosphere or submerged (section 2.2). Variable runs were designed to include longer  
193 wet runs, longer dry runs and wet and dry run of same duration and frequency. Control runs were non-  
194 variable and either constant wet (flood) or unsaturated and oxidised (field capacity). This allowed a  
195 comparison between variable and non-variable wet and dry runs. Constant flood and field capacity were  
196 sampled every week. Variable run samples were taken only at the start and end of a wet period. Runs  
197 were: 1 week wet followed by 1 week dry (1wwet), 1 week wet followed by 2 weeks dry (2wdry), 1 week  
198 wet followed by 3 weeks dry (3wdry), 2 weeks wet followed by 1 week dry (2wwet), 3 weeks wet followed  
199 by 1 week dry (3wwet), Flood (Flood) and field capacity (F/C). The temperature was maintained at 22-  
200 23°C for the 1<sup>st</sup> mesocosm experiment and ~18°C for the 2<sup>nd</sup> mesocosm experiment.

201 Water samples were taken from the top of the mesocosm using a plastic syringe and from the bottom  
202 via a tap, in that order to avoid mixing between levels and filtered through a 0.45 µm PTFE syringe filter.  
203 A Hanna Combo pH/EC and temperature hand held stick meter model No 98129, recorded pH,  
204 conductivity and temperature for each sample. An Aquaread Aquameter multiparameter water quality  
205 probe was used to measure dissolved oxygen (DO) and redox potential (ORP) (2<sup>nd</sup> mesocosm  
206 experiment only). The ORP reference electrode was type 3MPK1 AgCl and ORP readings were  
207 converted to the hydrogen scale (Eh) as instructed by Aquaread. For further detail regarding mesocosm  
208 methodology, please see Lynch et al. (2017).

209

210



211

212

213 Fig. 2 Outline of mesocosm including sampling points

214 Note: *Filtered samples are referred to as 'dissolved' concentrations. However, this is operationally*  
 215 *defined and the authors acknowledge that the samples may contain colloidal and/or nano-sized*  
 216 *particles.*

217 **2.4.2 Trace metal and anion analysis**

218 Flame Atomic Absorption Spectroscopy (FAAS) (Perkin Elmer Analyst 300) was used to measure Fe,  
 219 Mn, Pb, Ca, Ni, Cu ( $\text{mg l}^{-1}$ ) in filtered pore water samples from the 1<sup>st</sup> mesocosm experiment. Detection  
 220 limits were: Ca, 0.06; Fe, 0.03; Cu, 0.01; Mn, 0.01; Pb, 0.04 and Ni, 0.01 ( $\text{mg l}^{-1}$ ). Inductively Coupled  
 221 Plasma with Optical Emission Spectroscopy (ICP/OES) (iCAP 6500 Duo) was used to measure  
 222 dissolved Fe, Mn and Pb in (i) filtered pore water samples of the 2<sup>nd</sup> mesocosm experiment and (ii)  
 223 sequential extraction samples from the 1<sup>st</sup> and 2<sup>nd</sup> mesocosm experiments. Detection limits were: Fe,  
 224 0.005; Mn, 0.001; Pb, 0.05 ( $\text{mg l}^{-1}$ ). Ion Chromatography (Dionex ICS2000) was used to measure  
 225 dissolved sulphate, nitrate, chloride and phosphate in pore water samples of the 1<sup>st</sup> mesocosm  
 226 experiment and the 2<sup>nd</sup> mesocosm experiment. Detection limits were: sulphate, 0.07; nitrate, 0.04;  
 227 chloride, 0.06; phosphate, 0.06 ( $\text{mg l}^{-1}$ ). Flame photometer BWB technologies was used for detection  
 228 of Na, K and Ca in filtered pore water of the 2<sup>nd</sup> mesocosm experiment. For all analysis quality control  
 229 standards and blanks, either de-ionised water, or matrix matched solutions for sequential extractions,  
 230 were used throughout. The results were considered acceptable if the data were within 5% of the  
 231 expected concentration.

232

233 **2.4.3 Alkalinity and inorganic carbon analysis (water and sediments)**

234 Unfiltered water samples from both mesocosm treatment runs were analysed for alkalinity (as calcium  
235 carbonate) using the standard operating procedure for Great Lakes National Program office total  
236 alkalinity titration method (US EPA 1992). Filtered pore water samples were tested for total carbon (TC)  
237 and non purgeable organic carbon (NPOC) using a carbon analyser (Shimadzu TOC-V CSN). Inorganic  
238 Carbon = Total Carbon – Non Purgeable Organic carbon. For non purgeable organic carbon the sample  
239 was first acidified to pH 2 to transform inorganic carbon to CO<sub>2</sub>. The CO<sub>2</sub> was removed via sparging  
240 with a carrier gas. During this process some purgeable organic carbon (benzene, toluene, cyclohexane  
241 and chloroform) may be partly removed. Although there tends to be negligible amounts of these in  
242 surface water samples, the remaining organic carbon is “non-purgeable” and is measured, as mg (of  
243 carbon) per litre of water, through CO<sub>2</sub> detection in the analyser using a non-dispersive infrared (NDIR)  
244 detector. Standards and blanks were used throughout. The results were considered acceptable if within  
245 5% of the expected concentration. Sediment collected for the 2<sup>nd</sup> mesocosm experiment was analysed  
246 for total inorganic (IC) using a separate solid sample module of the Shimadzu instrument (SSM 5000A).  
247 A sub sample of sieved (2 mm) sediment was weighed (no greater than 50 mg), and oven dried at  
248 140°C for 24 hours. The sample was treated with phosphoric acid inside the Shimadzu instrument to  
249 produce CO<sub>2</sub> that was purged at 200°C and detected using a non-dispersive infrared (NDIR) detector.  
250 Calibration was performed using different weights of sodium carbonate containing 11.3% carbon. The  
251 results provided % TIC (Shimadzu Scientific Instruments, 2014). The results were considered  
252 acceptable if within 5% of the expected concentration.

253

254 **2.4.4 Statistical analysis**

255 All calculations were performed using SPSS 20.0. Statistical tests revealed the data was not normally  
256 distributed therefore significant differences in pore water data were identified through non-parametric  
257 Wilcoxon rank sum test. Relationships between Pb and pore water variables were determined using  
258 Spearman’s rho 2-tailed non-directional tests.

259

260 To determine key factors linked to the mobilization of dissolved Pb for selected variable runs at the  
261 bottom of the mesocosms, Principal Component Analysis (PCA) was carried out. Data was assessed  
262 to ensure (i) that underlying variables correlated (Bartlett’s test of sphericity) and (ii) sampling adequacy

263 (Kaiser-Meyer-Olkin). Factor rotation was chosen based on whether the factors (principal components  
264 (PC)) were thought to be unrelated (orthogonal) or related (oblique). For further information on PCA  
265 see supplementary information D.

266

#### 267 **2.4.5 PHREEQC (Ph-Redox-Equilibrium in “C”)**

268 The geochemical computer program PHREEQC was used for speciation and saturation index (SI)  
269 calculations using the WATEQ4F.dat database distributed with the PHREEQC program. The saturation  
270 state of various minerals were calculated using input data derived from pore water measurements for  
271 selected runs (Tables A1 and A2). Data was considered acceptable if charge balance was  $\leq 5\%$ .

272

273 In some cases the control of trace metal solutes by equilibrium with a mineral can be demonstrated  
274 (Appelo and Postma, 2010). The keyword ‘equilibrium\_phases’ was used to calculate the concentration  
275 of anglesite that would precipitate and subsequent dissolved Pb concentrations in pore and surface  
276 water if conditions were brought to equilibrium and reached saturation with respect to anglesite.

277

#### 278 **2.4.6 Sequential Extraction of sediment samples**

279 Dynamic changes in redox potential conditions can occur within river bank sediment due to flooding /  
280 draining sequences (Lynch et al 2017; Lynch et al. 2014; Du Laing et al. 2009). Different Fe phases  
281 display a wide range of reactivity (adsorption capacity and susceptibility to reduction). A fall in redox  
282 potential conditions can result in the microbially mediated reductive dissolution of Fe and Mn  
283 (hydroxides) (Stumm and Sulzberger 1992; Lynch et al. 2014). This can serve to remobilize  
284 partitioned contaminants such as Pb (Torres et al. 2013). When flood waters subside the exposure of  
285 previously reduced sediment surfaces to atmospheric conditions may result in the oxidation and  
286 hydrolysis of previously reduced Fe and Mn (Lovley and Phillips 1989; Grundl and Delwiche 1993). Fe  
287 and Mn (hydr)oxides can rapidly (minutes to hours) scavenge high concentrations of dissolved trace  
288 metal contaminants such as Pb (Burton 2010, Caetano et al. 2003). In order to understand the  
289 reactivity of Fe and Mn minerals in the sediment along with partitioned Pb and therefore the potential  
290 for the sediment to control the mobilisation of Pb in response to dynamic changes in redox potential a  
291 modified 4 step sequential extraction procedure was carried out in triplicate on sediments samples  
292 collected for 1<sup>st</sup> and 2<sup>nd</sup> mesocosm experiments. The sequential extraction procedure focused

293 primarily on Fe and Mn minerals with steps run sequentially from 'most reactive' to 'least reactive'.  
 294 Extractions were carried out on freeze dried -70°C sediment ( $63 \leq \mu\text{m}$ ) (Table 1). Please see  
 295 supplementary information 'E' for full extraction methodology.

296

297 Table 1 Sequential extraction steps

Step #	Extractant	Extraction details	References
1	0.5M HCl*	Rotational shaker for 1 hour, centrifuged, supernatant filtered (0.45 $\mu\text{m}$ )	Lovley and Phillips (1986)
2	0.25M hydroxylamine hydrochloride in 0.25M HCl	Rotational shaker for 1 hour, centrifuged, supernatant filtered (0.45 $\mu\text{m}$ )	Poulton and Cranfield (2005)
3	50 gL <sup>-1</sup> sodium dithionate with 0.2M in 0.35M acetic acid	Rotational shaker for 2 hours, centrifuged, supernatant filtered (0.45 $\mu\text{m}$ )	Poulton and Cranfield (2005)
4	Aqua Regia cHCl and cHNO <sub>3</sub> (3:1 molar ratio)	Agitated gently overnight. Following day heated 80 °C for 2 hours. Filtered Whatman no 42	Wilson and Pyatt (2007), Montserrat (2012)

298

299

300 **\*0.5M HCl is a moderately corrosive first step and therefore it is not possible to differentiate the**  
 301 **release of divalent ions from loosely sorbed/ exchangeable phase or as a result of dissolution**  
 302 **of amorphous or soluble phases. Furthermore, the first step was originally used for analysis of**  
 303 **Fe from within a different sediment environment. The implications regarding these points are**  
 304 **included in the results/ discussion sections as the authors consider the results provide valuable**  
 305 **supporting data.**

306

#### 307 2.4.7 Scanning Electron Microscopy with Energy Dispersive X-ray Spectroscopy (SEM/EDX)

308 A combination of SEM/EDX was carried out to create images of and identify elements at the surface of  
 309 the sediment samples for areas at micron scale. Freeze dried sediment was dusted lightly onto carbon  
 310 stubs and coated in carbon to encourage conductivity. Samples were analysed with a Philips XL30 FEG  
 311 ESEM fitted with an Oxford Instruments X-Sight EDS ATW X-Ray detector. Please see supplementary  
 312 data 'F' for full methodology.

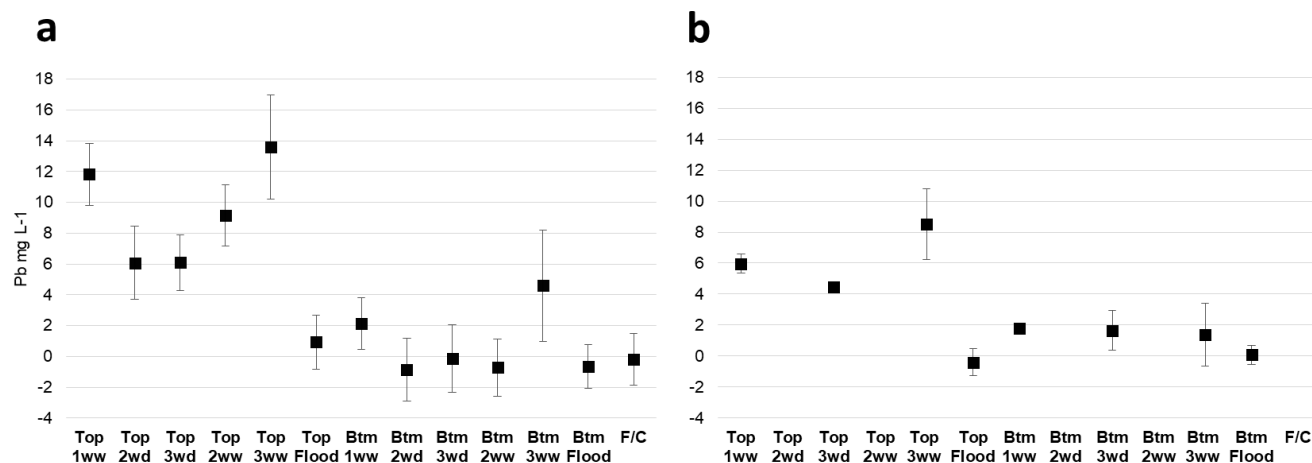
313 **3. Results and discussion**

314 **3.1 Factors influencing the mobilisation of dissolved Pb**

315 A key objective of the current study was to determine whether mining contaminated sediments became  
316 a source of dissolved Pb in response to flooding and draining sequences. The results indicated that  
317 these perturbations did influence the mobilisation of dissolved Pb, although patterns in the release of  
318 dissolved Pb were found to vary depending on the flood/drain sequence and the location (top/bottom)  
319 within the mesocosms.

320

321 The average concentration of dissolved Pb released over a flood period was significantly higher at the  
322 top of the mesocosm compared to the bottom ( $z = -7.3$ ,  $p = < 0.001$ ), ( $z = -2.525$ ,  $p = < 0.05$ ), 1<sup>st</sup> and  
323 2<sup>nd</sup> mesocosm experiments respectively. At the top of the mesocosm, within surface water, the  
324 concentration of dissolved Pb increased over the duration of the flood. All variable wet and dry runs  
325 displayed significantly higher concentrations of dissolved Pb at the end of a flood compared to the  
326 start ( $z = < -1.96$ ,  $p = < 0.05$ ) (Figs 3a and 3b). In contrast, at the bottom of the mesocosm almost all  
327 of the dissolved Pb was released at the start of a flood (within 2-3 hours) and concentrations  
328 remained relatively constant, or declined over the flood period. There was no significant increase in  
329 dissolved Pb between the start and end of a flood period at the bottom of the mesocosm for the  
330 2wdry, 3wdry, 2wwet and F/C runs ( $z = > -1.96$ ,  $p = > 0.05$ ), nor for the constant flood runs at the top  
331 ( $z = -0.73$ ,  $p = .465$ ) ( $z = -1.424$ ,  $p = 0.155$ ) and bottom ( $z = -0.63$ ,  $p = .53$ ) ( $z = -0.316$ ,  $p = 0.752$ ) of  
332 the 1<sup>st</sup> and 2<sup>nd</sup> mesocosm experiments respectively (Figs 3a and 3b). Similarities in the patterns of  
333 dissolved Pb release were apparent between the two mesocosm experiments possibly indicating the  
334 key geochemical mechanisms controlling Pb mobilisation were the same.



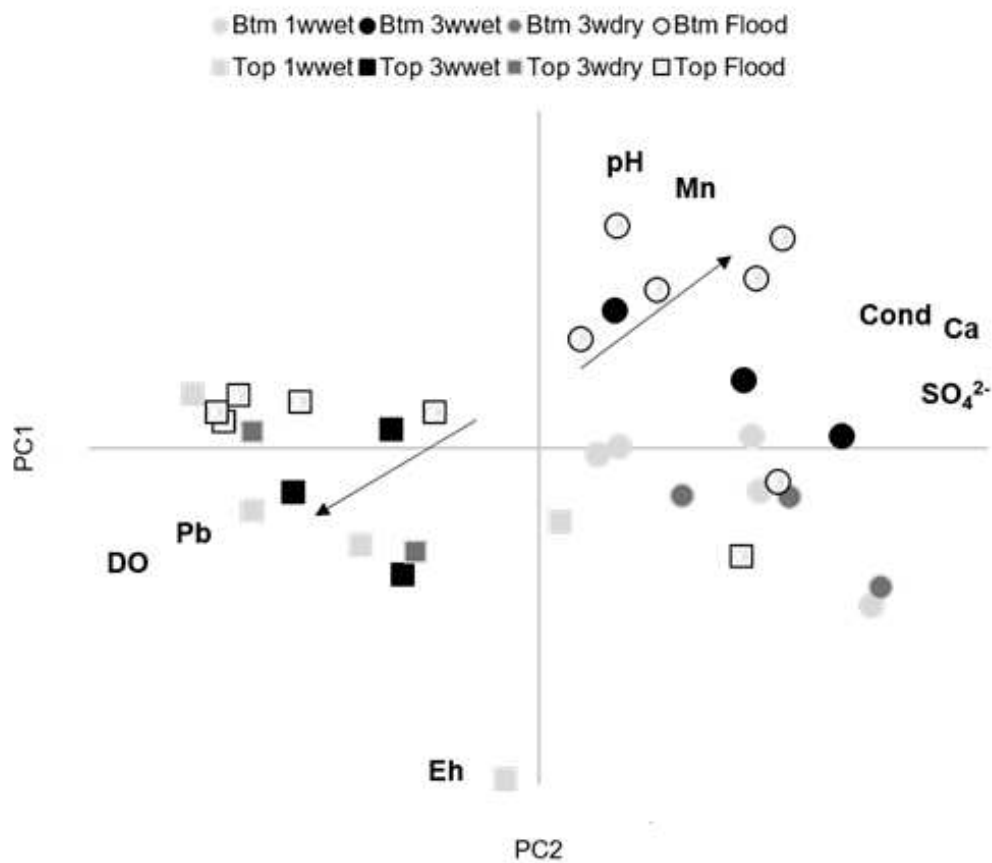
335  
 336 Fig. 3. Average concentration of dissolved Pb released over a flood period ( $\text{mg L}^{-1}$ ) (concentration at  
 337 the end of a flood minus concentration at the start) for all runs, top and bottom of the mesocosm for  
 338 (a) 1<sup>st</sup> mesocosm experiment, bars indicate standard error ( $n=9$  for 3wwet and 3wd,  $n = 12$  for 2ww  
 339 and 2wd,  $n = 18$  for 1ww, flood and F/C) (b) 2<sup>nd</sup> mesocosm experiment bars indicate standard error  
 340 ( $n=3$  for 3wwet and 3wd,  $n = 5$  for 1ww, flood). Principal components analysis was conducted on 8  
 341 items with orthogonal rotation (varimax) to determine the underlying factors influencing the  
 342 mobilisation of Pb. Two PCs had eigenvalues greater than '1': PC1 explained 62.7% and PC2  
 343 explained 14.9% of the variance. PC1 showed a high positive loading for sulphate (0.958) and Ca  
 344 (0.897) and a negative loading for Pb (-0.527). At the bottom of the mesocosms, runs with longer  
 345 flood periods, particularly the constant flood run, scored highly against this component (Fig. 4). Pore  
 346 and surface water chemical analysis found that average concentrations of dissolved sulphate and Ca  
 347 were higher at the bottom of the mesocosms compared to the top (Tables 2 and 3) and correlation  
 348 analysis for the flood run at the bottom of the mesocosm showed a significant negative relationship  
 349 between Pb and sulphate ( $r = -.889$ ,  $p = <.01$ ) and Pb and Ca ( $r = -.605$ ,  $p = <.01$ ). These results  
 350 could indicate that underlying factors contributing to the release of sulphate and Ca over flooded  
 351 periods may be linked to the lower concentrations of Pb at the bottom of the mesocosms. Inorganic  
 352 carbon (IC) in the sediment was below detection in the current study both prior to treatment and at the  
 353 end of the run. Pore and surface water analysis indicated that bicarbonate concentrations were  
 354 undetectable. Furthermore, it can be seen, section 3.2, Table 4, geochemical modelling, that no  
 355 carbonate minerals were predicted to precipitate. Therefore it is unlikely the substitution of Ca for Pb  
 356 in carbonate minerals such as calcite ( $\text{CaCO}_3$ ), aragonite ( $\text{CaMg}(\text{CO}_3)_2$ , and ankerite  
 357 ( $\text{Ca}(\text{Fe},\text{Mg})\text{CO}_3$ )<sub>2</sub> (Cravotta 2008; Fairchild et al. 2010) or the precipitation of Pb carbonate minerals

358 such as cerussite (VanLoon and Duffy, 2011) were key geochemical mechanisms controlling the  
359 mobilisation of dissolved Pb. Sulphate was present at higher concentrations than the other anions  
360 (nitrate, chloride and phosphate). In waters with high sulphate concentrations the production of  
361 hydrogen sulphide and precipitation of insoluble metal sulphide galena (PbS) can serve as a sink for  
362 dissolved Pb (Du Laing et al. 2009). However, although redox potential measurements were lower at  
363 the bottom of the mesocosms than at the top (Table 3), they did not decline low enough for the  
364 production of hydrogen sulphide (<120 mV) (Ross 1989; Gambrell et al. 1991; Bartlett 1999). Gypsum  
365 ( $\text{CaSO}_4 \cdot 2\text{H}_2\text{O}$ ) is often present in mining impacted catchments (Younger, 1998; Harris et al., 2003;  
366 Kuechler et al., 2004). Piper analysis indicated that the water samples were Ca-sulphate water type -  
367 typical of mine drainage. Dissolution of this mineral could account for the presence of sulphate and  
368 Ca in pore water and processes relating to the dissolution of this mineral could be linked to the  
369 attenuation of dissolved Pb. This is discussed further in section 3.2.

370 High negative loadings for DO (-0.814) and redox potential (-0.942) were recorded against PC1 and  
371 2. This is in line with the negative loading for Pb (-0.527) against PC1. Runs, at the top of the  
372 mesocosms, scored negatively against PC1 and in some cases PC2 (3wwet run) (Fig.4). DO and  
373 redox potential measurements showed conditions were oxic ~99.5% DO, Eh 494 mV at the top of the  
374 mesocosms (Table 3). These results indicate that underlying factors linked to high DO and redox  
375 potential conditions, may have contributed to releases of dissolved Pb over flood periods at the top of  
376 the mesocosms. Correlation analysis for the 3wwet run indicated a significant positive relationship  
377 between dissolved Pb and sulphate ( $r = .605$ ,  $p = <.01$ ) and dissolved Pb and Ca ( $r = .828$ ,  $p = <.01$ ).  
378 The oxidation of Pb sulphide minerals such as galena in mine tailings and contaminated sediment has  
379 been linked to the release of high concentrations of dissolved Pb into surface water during laboratory  
380 inundation experiments (Wragg and Palumbo-Roe 2011) and in the field, in response to storm events  
381 (Byrne et al 2012). The oxidation of galena would not necessarily produce excess acidity however,  
382 any subsequent hydrolysis (Younger 1998) or adsorption reaction (Dzombak and Morel 1987) would  
383 result in proton release. Therefore, the slightly acidic pH observed (pH 5.3, range 4.8 – 5.8), (pH 5.7,  
384 range 5.1 – 5.8) during the 1<sup>st</sup> and 2<sup>nd</sup> mesocosm experiments respectively could be linked to these  
385 acid producing processes and the poor buffering capacity of the water.

386





388

389 Fig. 4. Principal component analysis showing the distribution of pore water chemical samples along  
 390 the first two principal components includes runs 1wwet, 3wwet, 3wdry, flood at the top (squares) and  
 391 bottom (circles) of the mesocosms. Arrows indicate general trend for longer flooded runs (bottom)  
 392 compared to 1wwet and 3wwet runs (top) (2<sup>nd</sup> mesocosm experiment).

393  
394**Table 2: 1<sup>st</sup> mesocosm experiment, Mean and range (in parenthesis) of dissolved (<0.45µm) metals and anions (mg l<sup>-1</sup>), pH, Conductivity (µS/cm), Temperature (°C) at the end of a flood, by run, Top (T) and Bottom (B) of the mesocosm, key average values (bold and underlined), n=#<sup>1</sup>**

Run Location	1wwet (T) n=18	1wwet (B) n=18	2wdry (T) n=12	2wdry (B) n=12	3wdry (T) n=9	3wdry (B) n=9	2wwet (T) n=12	2wwet (B) n=12	3wwet (T) n=9	3wwet (B) n=9	Flood (T) n=33	Flood (B) n=33	F/C (B) n=33
<b>pH</b>	5.2	5.3	5.1	5.2	5.1	5.2	5.1	5.3	5.2	5.4	5.3	5.5	5.2
<b>(Range)</b>	(5 - 5.6)	(5.1 - 5.5)	(5 - 5.3)	(5.1 - 5.5)	(4.8 - 5.3)	(5 - 5.3)	(4.9 - 5.4)	(5.1 - 5.5)	(4.9 - 5.7)	(5.2 - 5.7)	(5 - 5.8)	(5 - 5.7)	(5.1 - 5.4)
<b>Temp</b>	22.3	23.1	22.3	23.0	23.0	23.8	22.6	23.3	22.0	22.7	22.4	23.1	22.9
<b>(Range)</b>	(20.9 - 24.2)	(21.9 - 24.8)	(21.2 - 23.3)	(21.7 - 23.9)	(21.4 - 24.4)	(22.3 - 25.1)	(20.4 - 24.5)	(20.9 - 25.1)	(21.4 - 22.6)	(22.1 - 23.2)	(19.9 - 24.5)	(29.9 - 25)	(21 - 25)
<b>Cond</b>	110.6	183.2	100.2	188.4	110.9	208.3	134.2	208.1	156.4	230.4	105.8	248.6	77.9
<b>(Range)</b>	(87 - 144)	(155 - 204)	(88 - 116)	(152 - 214)	(94 - 136)	(164 - 250)	(107 - 156)	(188 - 224)	(146 - 169)	(218 - 264)	(46 - 126)	(140 - 339)	(50 - 130)
<b>Fe</b>	0.0	0.4	0.0	0.6	0.0	0.2	0.0	3.0	0.0	6.0	0.0	8.9	0.0
<b>(Range)</b>	0.0	(0 - 1.7)	0.0	(0 - 1.6)	0.0	(0 - 0.8)	0.0	(2.2 - 3.9)	0.0	(3.6 - 10)	0.0	(0 - 27.7)	(0 - 0.5)
<b>Mn</b>	0.2	1.6	0.2	1.6	0.2	1.4	0.3	5.3	1.5	7.7	0.5	9.6	0.4
<b>(Range)</b>	(0.1 - 0.4)	(1.2 - 1.8)	(0.1 - 0.2)	(1.1 - 2.2)	(0.1 - 0.3)	(0.6 - 2.9)	(0 - 0.7)	(3.5 - 6.4)	(0.7 - 3.1)	(6.7 - 9.6)	(0 - 1.3)	(0.4 - 16.6)	(0 - 1)
<b>Pb</b>	17.1	14.1	15.4	13.9	14.3	12.6	18.5	13.2	<b><u>21.5</u></b>	14.4	17.2	<b><u>10.8</u></b>	10.2
<b>(Range)</b>	(9.8 - 22.3)	(8.6 - 24.3)	(13.2 - 17.2)	(12.5 - 15.2)	(10.8 - 16.8)	(10.6 - 16.1)	(14.7 - 24.4)	(10.1 - 13.2)	(16.7 - 30.6)	(9.7 - 24.7)	(5.2 - 27.2)	(3.9 - 28.5)	(4.2 - 23.7)
<b>Ca</b>	2.4	3.9	1.7	3.4	2.1	4.1	2.3	3.9	3.3	4.2	2.6	4.5	1.9
<b>(Range)</b>	(1.7 - 3.4)	(2.6 - 5)	(1.4 - 2.1)	(2.1 - 4.5)	(1.9 - 2.9)	(2.7 - 5.9)	(1.6 - 2.6)	(2.6 - 5)	(2.8 - 3.8)	(3.9 - 4.7)	(1.5 - 3.6)	(2.8 - 6.8)	(1.3 - 2.8)
<b>NO<sub>3</sub><sup>-</sup></b>	2.3	0.5	3.3	2.6	4.1	2.5	1.9	0.0	1.5	0.0	1.4	0.6	2.3
<b>(Range)</b>	(0 - 5.7)	(0 - 1.5)	(2 - 4.9)	(0 - 4.8)	(2.6 - 5.7)	(0 - 6)	(0.9 - 3)	0.0	(0 - 3.2)	0.0	(0 - 4.2)	(0 - 8.7)	(0.7 - 4.2)
<b>Cl<sup>-</sup></b>	1.5	1.2	1.5	1.3	2.3	1.9	2.0	1.3	2.0	1.3	2.0	2.0	1.8
<b>(Range)</b>	(0.3 - 2.9)	(0 - 2.5)	(0.9 - 2.8)	(0.8 - 2.4)	(1.6 - 3.2)	(1.3 - 2.7)	(0.9 - 3.1)	(0.5 - 2.2)	(0.9 - 2.5)	(0.7 - 1.9)	(1.1 - 3)	(0.8 - 3.9)	(0 - 17.8)
<b>SO<sub>4</sub><sup>2-</sup></b>	38.9	71.2	44.5	84.1	42.7	87.9	48.6	82.9	61.8	95.0	46.5	119.7	36.2
<b>(Range)</b>	(10.8 - 65)	(60.2 - 100.8)	(25.3 - 90.9)	(57.3 - 142.8)	(25.4 - 63.3)	(61.2-129.5)	(34.7 - 63.4)	(65.3 - 94.2)	(47.2 - 85)	(79.6 - 121.2)	(13.5 - 106.4)	(47.6 - 277.7)	(16.9 - 90.5)

395

<sup>1</sup> Note: 'n' relates to number of samples taken at the end of a flood period. The 'n' varied between runs because certain runs had more flood periods than others over the treatment period. Includes replicates.

396 **Table 3: 2<sup>nd</sup> mesocosm experiment, Mean and range (in parenthesis) of dissolved (<0.45µm)**  
 397 **metals and anions (mg L<sup>-1</sup>), pH, Conductivity (µS/cm), Temperature (°C), DOC (mg L<sup>-1</sup>), TIC (mg**  
 398 **L<sup>-1</sup>) at the end of a flood, by run, Top (T) and Bottom (B) of the mesocosm, key average values**  
 399 **(bold and underlined), n= #<sup>2</sup>**

	<b>1wwet (T)</b> <b>n=5</b>	<b>1wwet (B)</b> <b>n=5</b>	<b>3wdry (T)</b> <b>n = 3</b>	<b>3wdry (B)</b> <b>n = 3</b>	<b>3wwet (T)</b> <b>n = 3</b>	<b>3wwet (B)</b> <b>n = 3</b>	<b>flood (T)</b> <b>n = 10</b>	<b>Flood (B)</b> <b>n = 10</b>
<b>pH</b>	5.5	5.7	5.6	5.7	5.6	5.8	5.7	5.8
<b>(range)</b>	(5.1 - 5.7)	(5.6 - 5.8)	(5.5 - 5.7)	(5.6 - 5.7)	(5.4 - 5.7)	(5.7 - 5.8)	(5.4 - 5.8)	(5.6 - 5.8)
<b>Temp</b>	17.5	17.8	17.7	17.7	18.4	18.9	17.9	18.2
<b>(range)</b>	(16 - 20)	(16.4 - 20.1)	(16.2 - 20.3)	(16.3 - 20.3)	(17 - 19.6)	(17.5 - 20)	(16 - 20.3)	(16.5 - 20.3)
<b>Cond</b>	225.2	392	175.3333	382	230.6667	405	264.9	408.4
<b>(range)</b>	(148 - 373)	(336 - 435)	(170 - 186)	(338 - 415)	(206 - 276)	(359 - 436)	(162 - 416)	(342 - 452)
<b>D.O. %</b>	100	34	102	37	94	18	102	12
<b>(range)</b>	(78 - 109)	(10.4 - 43.2)	(99 - 105)	(13.1 - 52.7)	(80.5 - 101)	(8.3 - 28.1)	(98 - 111)	(7.8 - 23)
<b>Eh</b>	509	482	499	491	483	428	485	423
<b>(range)</b>	(459 - 603)	(456.9 - 530)	(479 - 525)	(478.9 - 509)	(468 - 504)	(412.7 - 436)	(446 - 555)	(381 - 485)
<b>Fe</b>	0.0	0.1	0.0	0.1	0.7	0.1	0.0	0.3
<b>(range)</b>	0.0	(0 - 0.1)	(0 - 0.1)	(0 - 0.2)	(0 - 2)	(0.1 - 0.2)	(0 - 0.2)	(0.1 - 0.6)
<b>Mn</b>	0.1	0.1	0.0	0.1	0.1	3.5	0.2	5.8
<b>(range)</b>	(0 - 0.1)	(0.1 - 0.2)	0.0	(0 - 0.2)	(0 - 0.1)	(2.2 - 5.3)	(0 - 0.7)	(1 - 10.1)
<b>Pb</b>	<b><u>8.3</u></b>	4.9	6.1	5.8	<b><u>10.0</u></b>	4.9	<b><u>8.6</u></b>	<b><u>3.8</u></b>
<b>(range)</b>	(8 - 9.2)	(3.8 - 5.6)	(5 - 6.7)	(4.3 - 7)	(7.5 - 14.2)	(2.3 - 6.9)	(5 - 15)	(1.7 - 4.8)
<b>Ca</b>	2.4	11.8	2.0	13.7	4.7	15.7	5.7	13.6
<b>(range)</b>	(0 - 8)	(8 - 14)	(0 - 4)	(16 - 12)	(3 - 7)	(14 - 17)	(0 - 18)	(4 - 19)
<b>Nitrate</b>	1.6	1.4	0.6	1.9	1.1	0.1	0.7	0.0
<b>(range)</b>	(0.2 - 2.8)	(0.6 - 2.3)	(0 - 1.2)	(1 - 2.5)	(0.4 - 1.7)	(0 - 0.2)	(0 - 2.1)	(0 - 0.5)
<b>Chloride</b>	8.5	3.3	1.7	2.6	4.0	3.5	7.8	6.0
<b>(range)</b>	(2.4 - 23.5)	(2.6 - 4.8)	(1.27 - 2.48)	(1.4 - 3.4)	(1.6 - 6.4)	(1.1 - 5.5)	(1.5 - 27.6)	(0.7 - 17.5)
<b>Sulphate</b>	25.3	95.2	17.7	120.3	36.0	110.3	35.5	94.6
<b>(range)</b>	(8.5 - 64)	(121.9 - 47.7)	(8.8 - 35.2)	(90 - 145)	(19.3 - 52.9)	(66.6 - 147.7)	(7 - 115)	(46 - 138)
<b>Na</b>	2.2	4.8	3.0	4.7	5.3	14.3	7.3	8.8
<b>(range)</b>	(0 - 4)	(3 - 7)	(1 - 6)	(3 - 7)	(4 - 7)	(9 - 19)	(1 - 22)	(2 - 18)
<b>K</b>	1.2	1.0	0.0	0.7	0.3	1.0	2.8	0.7
<b>(range)</b>	(0 - 4)	1.0	0.0	(0 - 1)	(0 - 1)	1.0	(0 - 25)	(0 - 1)
<b>DOC</b>	2.5	3.1	1.9	3.1	2.6	4.3	2.6	3.6
<b>(range)</b>	(2.1 - 3.2)	(2.4 - 3.5)	(1.9 - 2)	(2.6 - 3.8)	(1.9 - 3)	(3.7 - 4.9)	(1.9 - 4.9)	(2.5 - 4.8)
<b>TIC</b>	0.8	1.2	0.6	1.1	0.8	2.8	0.7	2.5
<b>(range)</b>	(0.4 - 1.1)	(0.6 - 1.8)	(0.3 - 0.9)	(0.7 - 1.6)	(0.7 - 1.1)	(2.3 - 3.4)	(0.2 - 1.4)	(1.1 - 4.3)

<sup>2</sup> Note: 'n' relates to number of samples taken at the end of a flood period. The 'n' varied between runs because certain runs had more flood periods than others over the treatment period.

400 **3.2 Solubility control of dissolved Pb concentrations in pore and surface water by equilibrium**  
 401 **with anglesite**

402 Anglesite has been reported to form as a weathering product from the oxidation of galena in mine  
 403 drainage environments (Harris et al. 2003; Palumbo-Roe et al 2013). To assess how close to  
 404 saturation the flood water solutions were with respect to mineral phases, particularly anglesite, that  
 405 may have formed over the treatment period, saturation indices (SI) were calculated using PHREEQC  
 406 (Ball and Nordstrom, 1991).

407 The three week wet run (top) and flood run (bottom) were selected for analysis because the highest  
 408 average concentration of dissolved Pb was observed for the 3wwet run at the top of the mesocosm  
 409 ( $21.5 \pm 2.9 \text{ mg l}^{-1}$ ), ( $10 \pm 2.1 \text{ mg l}^{-1}$ ) and the lowest average concentration was observed for the  
 410 constant flood run at the bottom ( $10.8 \pm 2 \text{ mg l}^{-1}$ ), ( $3.8 \pm 0.3 \text{ mg l}^{-1}$ ) (Tables 2 and 3). Mineral phases  
 411 and SI's were calculated from input data (Table A1) and are listed (Table 4).

412 **Table 4. Mineral Phases, SI and charge balance (%) (first mesocosm run)**

Week	D	H	L	D	H	L
Sample	3wwet	3wwet	3wwet	Flood	Flood	Flood
Location	Top	Top	Top	Bottom	Bottom	Bottom
Charge balance %	0.5	-0.8	-0.2	0.2	0	-0.1
Anglesite PbSO <sub>4</sub>	<b>0.36</b>	<b>0.25</b>	<b>0.32</b>	<b>0.37</b>	<b>0.04</b>	<b>-0.07</b>
Larnakite PbO:PbSO <sub>4</sub>	-1.58	-1.13	-1.52	-0.62	-1.41	-0.34
Pb(OH) <sub>2</sub>	-2.09	-2.05	-2.54	-1.65	-2.12	-1.95
Gypsum CaSO <sub>4</sub> .2H <sub>2</sub> O	-2.96	-3.02	-2.88	-2.72	-2.56	-2.46
Zincite ZnO	-4.94	-4.58	-5.06	-4.2	-4.12	-3.9
ZnO(a)	-4.96	-4.61	-5.03	-4.26	-4.2	-3.93
Bianchite ZnSO <sub>4</sub> :6H <sub>2</sub> O	-5.49	-5.28	-5.18	-5.18	-4.98	-5.02
ZnSO <sub>4</sub> :H <sub>2</sub> O	-6.76	-6.54	-6.47	-6.43	-6.22	-6.28
Melanterite FeSO <sub>4</sub> :7H <sub>2</sub> O	ND	ND	ND	-5.15	-4.63	-4.44
Pyrochroite Mn(OH) <sub>2</sub>	-9.89	-9.42	-9.77	-8.41	-8.17	-7.77
Birnessite MnO <sub>2</sub>	-20.09	-19.43	-20.17	-18.02	-17.77	-16.97

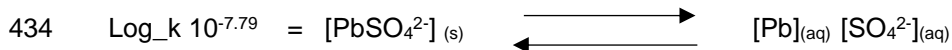
413 Note: All solution output results were checked for charge balance (within 5%). Small concentrations of Na were added to make  
 414 up for any charge imbalance. Na was not measured in the pore water, however concentrations measured in previous studies at  
 415 the sample site (Montserrat, 2010) were similar to the concentrations used to balance charges (7.5 – 32 mg/L). ND= no data/  
 416 dissolved Fe was below detection.

417 For both the 3 week wet (top) and constant flood (bottom) runs, surface and pore water conditions  
418 reached supersaturation with respect to anglesite by the end of the first 3 week flood (week D) (Table  
419 4). For the constant flood run, pore water conditions then changed from supersaturated to saturated  
420 by weeks H and L. This was not the case for the 3 week wet run where conditions remained  
421 supersaturated over the entire treatment period.

422 The flood run, unlike the variable runs, was not periodically drained and exposed to atmospheric  
423 conditions. The sediment, to a large extent, remained saturated and the water stagnant so it is  
424 possible that this system could have moved towards an equilibrium state.

425 To test that theory, a simple script was run using PHREEQC to calculate the anglesite precipitation  
426 that would occur if the input data (Table A1) for sample weeks D, H, L reached saturation with respect  
427 to anglesite. The program also calculated the concentration of dissolved Pb that would be expected in  
428 pore water under these new saturated conditions (Fig 5). The script was run for both the flood run  
429 (btm) and 3wwet run (top) for comparison.

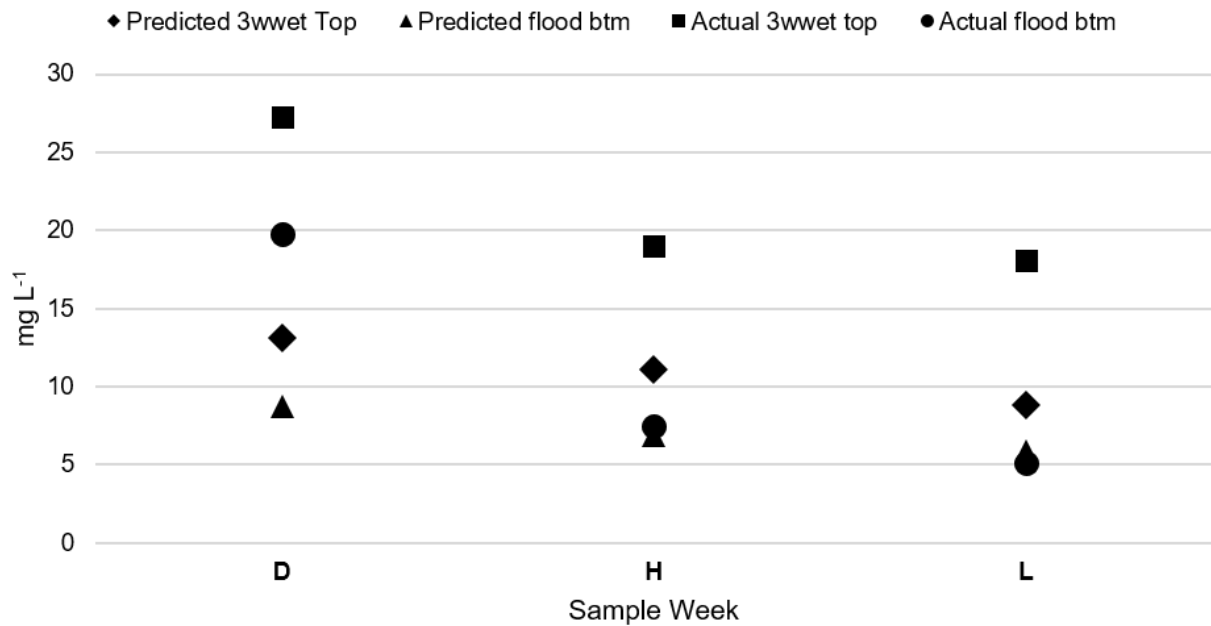
430 In theory, if pore water conditions reach supersaturation with respect to anglesite, as was found to  
431 occur for the 3 week wet and constant flood run (week D), according to Le Châtelier's principle  
432 anglesite precipitation would occur and result in the decline in dissolved Pb and sulphate  
433 concentrations.



435 For the flood run, week D, conditions were supersaturated with respect to anglesite (Table 4). Actual  
436 concentrations of Pb were higher in pore water than the concentrations predicted at equilibrium with  
437 respect to anglesite (Fig 5). By week L pore water conditions were no longer supersaturated (Table 4)  
438 and actual Pb concentrations had declined to 5mg/L (Fig 5). Predicted Pb concentrations at  
439 equilibrium for the flood run, weeks H and L were similar to actual Pb concentrations for these weeks  
440 (Fig 5), indicating that conditions had moved towards an equilibrium state.

441

442



443

444 Fig 5. Concentrations of dissolved Pb measured (actual) in pore and surface water and calculated  
 445 (predicted) by bringing the system to saturation with respect to anglesite for the 3wwet (top) and flood  
 446 run (bottom) of the mesocosms (1<sup>st</sup> mesocosm experiment).

447 Predicted Pb concentrations for the 3wwet run at the top of the mesocosm were lower than actual Pb  
 448 concentrations (Fig 5). For this run, conditions reached supersaturation at the end of a three week  
 449 flood and anglesite precipitation was predicted to occur but the actual Pb concentration data shows  
 450 that this process did not result in a decline in dissolved Pb concentrations. The results indicate that  
 451 the system was not in equilibrium and the solubility of anglesite had little control over dissolved Pb  
 452 concentrations at the top of the mesocosms. For the 3wwet run long flood periods were followed by  
 453 short drainage periods and re-flooded though addition of fresh artificial rain water. Sediment would  
 454 therefore have been exposed to oxic conditions (particularly at the surface) that would have  
 455 encouraged oxidation of Pb sulphide minerals and release of dissolved Pb during periods of  
 456 inundation.

457 Concentrations of dissolved Pb were observed to be lower in the second mesocosm experiment  
 458 however saturation indices calculated for the 2<sup>nd</sup> mesocosm experiment using information from input  
 459 Table A2 showed that conditions at the bottom of the mesocosm were saturated with respect to  
 460 anglesite (Table B1). The high concentration of sulphate measured at the bottom of the mesocosms  
 461 during this experiment (Table 3) would have influenced saturation indices for anglesite. The  
 462 dissolution of sulphate bearing minerals such as gypsum may have contributed to the high sulphate

463 concentrations at the bottom of the mesocosms. SI calculations indicated gypsum was  
464 undersaturated, conditions that would favour the dissolution of this mineral. Batch-type experiments  
465 investigating the interaction of gypsum with Pb in aqueous solutions observed the rapid dissolution of  
466 gypsum and simultaneous formation of anglesite on the gypsum surface and in solution (Astillerox et  
467 al. 2010). In the current study sulphate producing mechanisms such as dissolution of soluble  
468 sulphates would have encouraged the rapid precipitation of anglesite and provided a solubility control  
469 over dissolved Pb concentrations at the bottom of the mesocosm. Conditions were just below  
470 saturation with respect to anglesite at the top of the mesocosm (Table B1) and therefore it is likely the  
471 solubility of anglesite had little control over dissolved Pb concentrations at the top of the mesocosms  
472 for the 2nd mesocosm run.

### 473 **3.3 Sediment analysis**

474 Fe and Mn minerals have been reported as volumetrically the most important contaminant hosts in  
475 metal mining contaminated sediment in England and Wales (Hudson-Edwards 2003). Reactive 'easily  
476 reducible' Fe and Mn (hydr)oxides have been found to reduce more quickly (Lovley and Phillips 1987)  
477 at a higher redox potential (Du Laing et al. 2009) than older more crystalline forms such as goethite or  
478 hematite. Many studies have observed the partitioning of Pb with Fe and Mn hydroxides in metal  
479 contaminated sediments (Macklin and Dowsett 1989; Evans 1991; Hudson-Edwards 2003; Burton et  
480 al. 2005; Byrne et al. 2010; Farnsworth and Herring 2011). Dynamic changes in redox potential  
481 conditions and pH can bring about the reductive dissolution and precipitation of Fe and Mn hydroxides  
482 (Lovley and Philips 1986; Lee et al. 2002) and that can control the mobilisation of Pb (Charlatchka  
483 and Cambier 2000; Lesven et al. 2010).

484 Extraction step 1 was intended to remove reduced Fe, Mn and Pb loosely sorbed to the sediment  
485 surface and extraction step 2 was expected to recover easily reducible Fe and Mn (hydr)oxides along  
486 with any partitioned Pb. The first two extractions therefore represented the most labile forms of Fe  
487 and Mn. A control standard of ferrihydrite was synthesised using Poulton and Cranfield (2005)  
488 methodology and showed a 77% Fe recovery during extraction step 1. It is therefore likely that high  
489 concentrations of 'easily reducible' Fe were extracted during step 1. However, it can be seen from the  
490 results (Table 5) that relatively small concentrations of Fe and Mn were extracted from the sediment  
491 during the 1<sup>st</sup> and 2<sup>nd</sup> extractions compared to Pb. Almost all of the Pb (> 90%) was extracted during

492 the first 2 extraction steps (Fig. 6). The first extraction step was originally carried out on tidal river  
 493 surface sediment (Lovley and Phillips 1986). Sediment was not severely Pb-contaminated and  
 494 sulphate concentrations were in some cases an order of magnitude lower compared to the current  
 495 study. Although chemical extractions are intended to be phase specific total specificity is highly  
 496 unlikely (Leinz et al. 2000; Linge, 2008). Baba et al. (2011) reported that a 0.5 M HCl extraction  
 497 resulted in 30% Pb removal from an anglesite sample (< 63 µm) within 1 hour. Leinz et al. (2000)  
 498 carried out a series of Tessier et al. (1979) extractions and reported a 60,000 mg/kg recovery of Pb  
 499 from anglesite using an extraction of 0.25 M hydroxylamine hydrochloride in 0.25 M HCl for 30  
 500 minutes at 50°C. Furthermore, 0.5 M HCl produces a low pH extraction and galena dissolution has  
 501 been found to increase as pH declines (Cama et al. 2005). It is possible therefore the high  
 502 concentration of Pb released during the 1<sup>st</sup> and 2<sup>nd</sup> extraction may be due, in part, to the presence of  
 503 other minerals, such as galena or anglesite in the sediment. The presence of these minerals was  
 504 corroborated through SEM/EDX analysis (Figs 8-10, Table 6.).

505 **Table 5 Mean concentrations (mg kg<sup>-1</sup>) of metals in sediment (< 63 µm grain size) collected in**  
 506 **2012 and 2014 (n=3). Results are shown for pseudo-total metals and each geochemical phase**  
 507 **of the sequential extraction.**

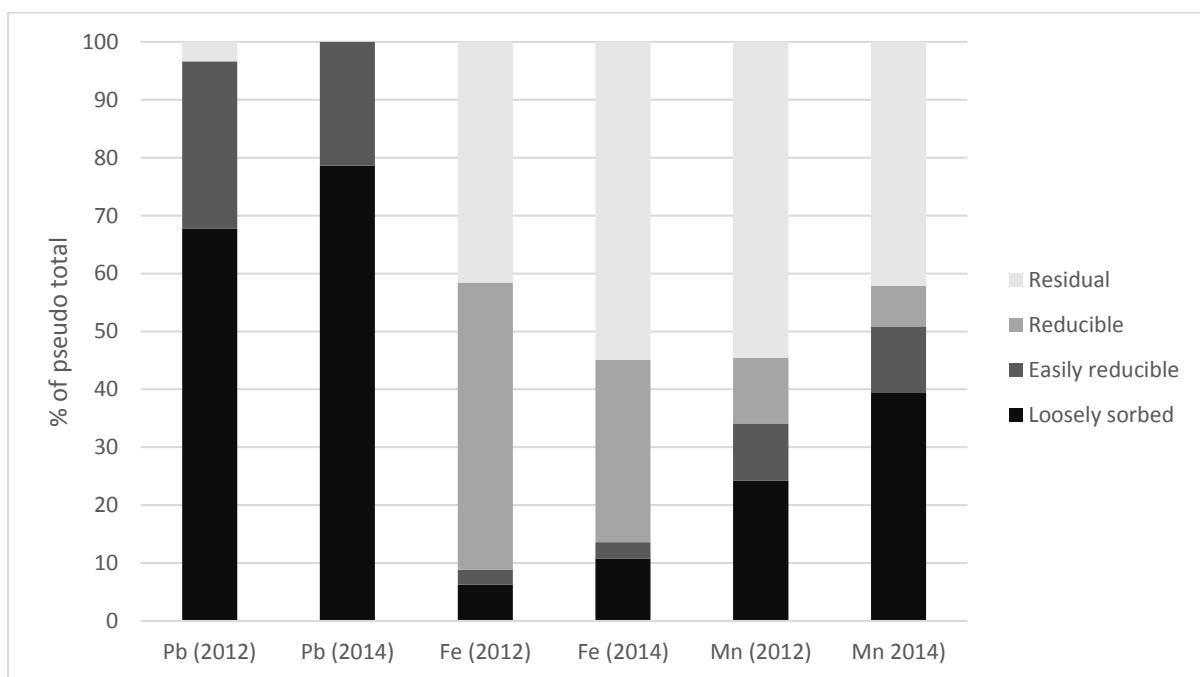
	Pb (2012)	Pb (2014)	Fe (2012)	Fe (2014)	Mn (2012)	Mn (2014)
Loosely sorbed	59,463.9 ±8589.6	59,807.2 ±2015.1	2,905.4 ±242.3	4,721.7 ±49.2	146.9 ±13.5	361.3 ±2.3
Easily reducible	25,306.4 ±3940.23	16,276.9 ±911.9	1,183.8 ±76.7	1,255.5 ±111.3	59.9 ±9.2	105.5 ±10.8
Reducible	0	0	22,973.3 ±1596.4	13,812.6 ±248.1	68.8 ±3.6	64.5 ±0.8
Residual	2952.9 ±1436.2	0	19,260.6 ±1452.8	24,078.5 ±990.6	330.9 ±24.2	386.4 ±15.1
Pseudo total	87,723.2	76,084.1	46,323.1	43,868.3	606.4	917.7
EA PEL guidelines *	91.3	91.3				

508

509 In the current study concentrations of dissolved Fe were very low in surface and pore water compared  
 510 to other metals (Table 2 and 3). Gotoh and Patrick (1974) found that under flooded conditions Fe



511 (hydr)oxide reductive dissolution occurred at 300 mV (pH 5), therefore this mechanism was unlikely to  
 512 occur in the present study as redox potential measurements did not decline low enough, even at the  
 513 bottom of the mesocosms. Furthermore microbial depletion of oxygen is limited by the availability of  
 514 labile organic carbon (Gambrell et al. 1991) and the low-medium organic carbon measured in the  
 515 current study would be unlikely to favour a large fall in redox potential conditions. The results of  
 516 sediment and water analysis indicate that it is unlikely co-precipitation of Pb with Fe and Mn  
 517 (hydr)oxides followed by reductive dissolution would have been a key mechanism controlling the  
 518 mobilisation of Pb.

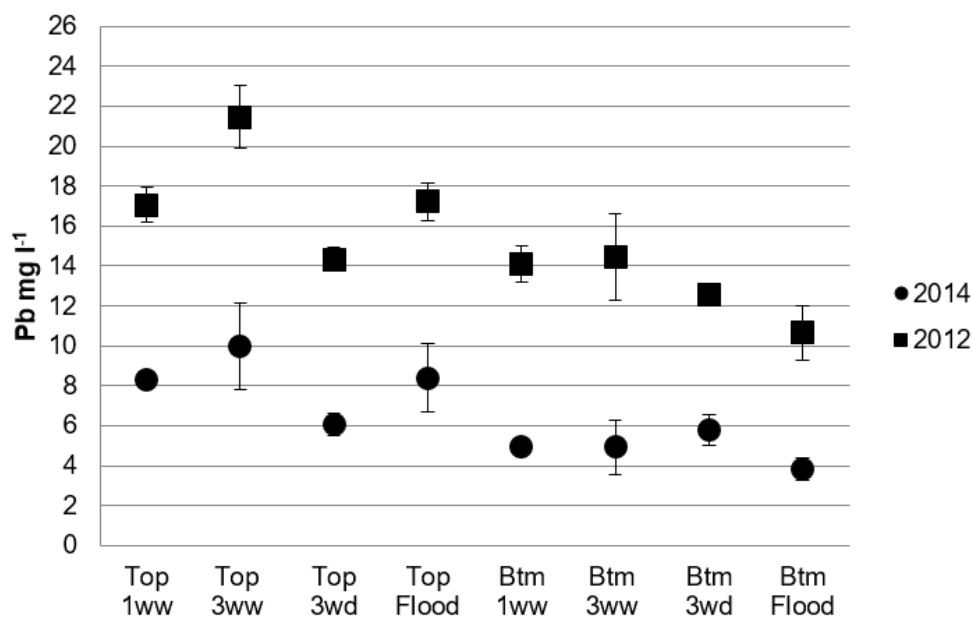


519 Fig 6. Mean sequential extraction and residual Pb, Fe and Mn concentrations (n = 3) in the sediment  
 520 (< 63 μm grain size) collected in 2012 and 2014. Results are shown as percentages associated with  
 521 each phase  
 522

523 Higher concentrations of Pb were found in the 'easily reducible' fraction of the sediment sampled  
 524 during the 1<sup>st</sup> mesocosm run, compared to the 2<sup>nd</sup> (Table 5) and it is likely that differences in Pb  
 525 concentration in the sediment were reflected in pore water concentrations (Fig. 7). The average  
 526 concentration of 'dissolved' Pb was significantly lower for 2<sup>nd</sup> mesocosm experiment in 2014  
 527 compared to the 1<sup>st</sup> experiment in 2012 for all runs at the top and bottom of the mesocosm ( $z = -$   
 528  $1.96$ ,  $p < 0.05$ ). Average concentrations were approximately 2 – 3 times lower (Fig. 7). Sediment  
 529 collected in 2012 was taken from piles of mine tailings that had been dumped along the side of the  
 530 river due to inefficient processes at the time of extraction. This waste would contain high

531 concentrations of the original ore minerals and their oxidised products. In 2014 sediment was  
 532 collected from a different riverbank location closer to the river channel. This sediment may have been  
 533 deposited during overbank flooding and as wash load transported from waste piles surrounding the  
 534 site, this process has been described by (Merrington and Alloway 1994). The spatial heterogeneity of  
 535 the post mining landscape is problematic with regards to predicting diffuse pollution. The above  
 536 results highlight the importance of characterising the sediment within a catchment prior to modelling  
 537 pollutant releases.

538

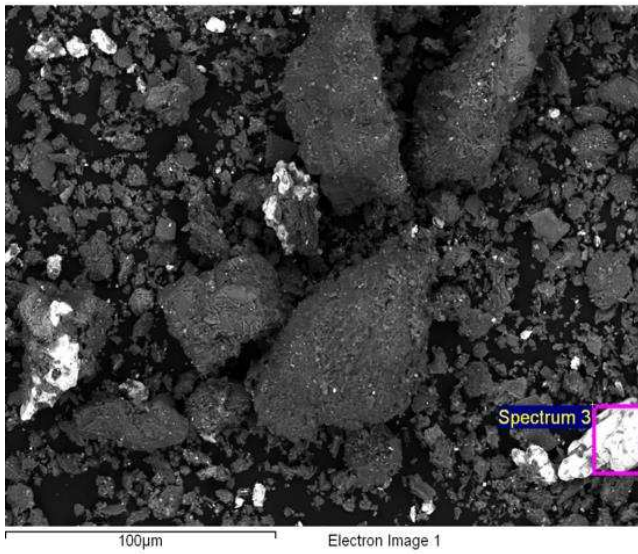


539

540 Fig 7. Average concentration (mg l<sup>-1</sup>) of dissolved Pb released at the end of a flood for mesocosm  
 541 experiments in 2012 and 2014 by run at the top and bottom. Bars indicate standard error 1st  
 542 mesocosm experiment n=9 for 3wwet and 3wd, n = 12 for 2ww and 2wd, n = 18 for 1ww, flood and  
 543 F/C; 2nd mesocosm experiment n=3 for 3wwet and 3wd, n = 5 for 1ww, flood.

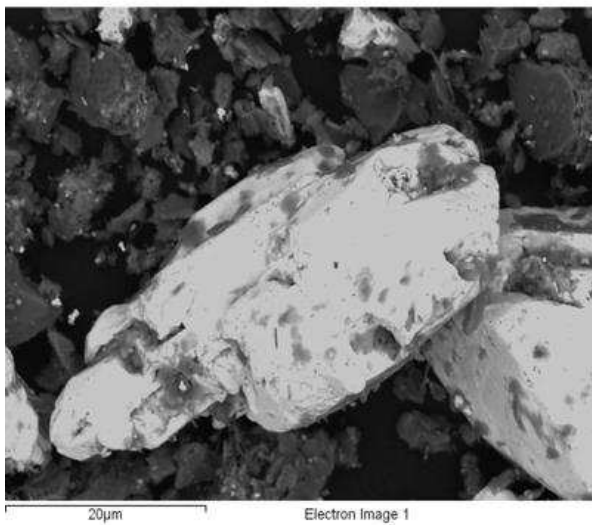
544 SEM/EDX analysis was carried out to identify possible mineral associations of Pb in the sediment.

545 Fig. 8 shows a back scattered electron image of the sediment (1st mesocosm run). Heavy elements  
 546 (high atomic number) backscatter electrons more strongly than light elements (low atomic number)  
 547 and therefore appear brighter in the image. As Pb is considered a heavier element, a bright grain was  
 548 selected for analysis (spectrum 3) and a magnified back scattered electron image taken (Fig. 9).



549

550 Fig. 8 Back scattered electron image of sediment (1st mesocosm run)



551

552 Fig. 9. Magnified Back scattered electron image of the grain in spectrum 3

553 EDX was carried out and the resulting quant specification (Table 6) shows an atomic % close to 1:1  
 554 ratio for Pb and S which could possibly indicate the presence of the mineral galena.

555 Table 6. Quant specification for spectrum 3

Element	Weight%	Atomic%

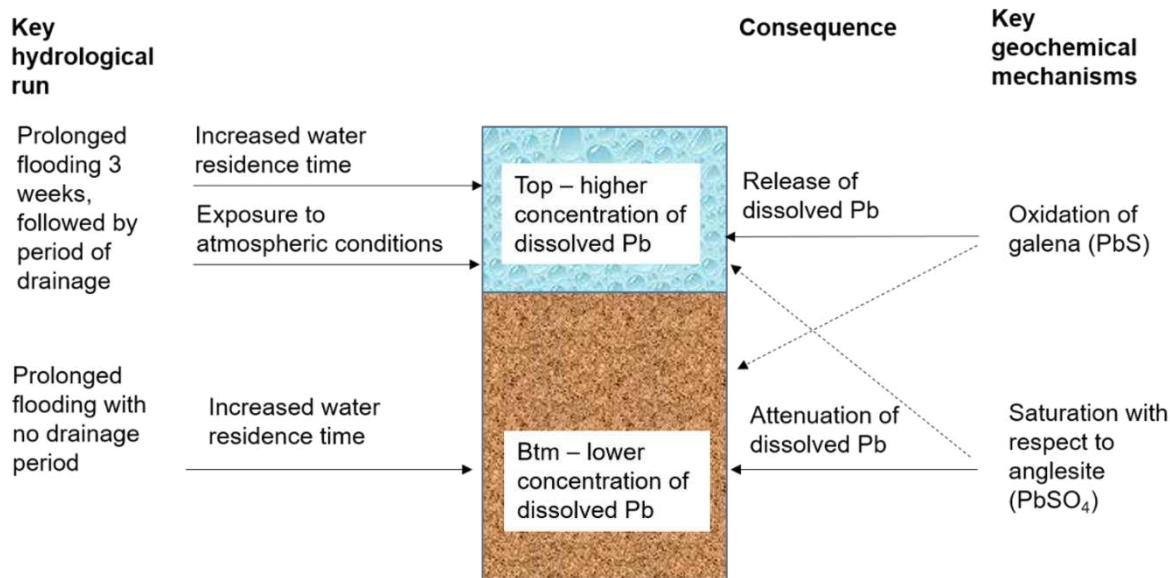
S K	13.13	<b>45.43</b>
Mn K	-0.07	-0.14
Fe K	2.85	5.65
Zn L	3.46	5.87
Pb M	80.64	<b>43.19</b>
Totals	100.00	

556

557 The smart map pattern (See supplementary data 'G') for elements Pb, S and Fe shows that the grain  
558 in spectrum 3 is likely to be a Pb, S mineral. A similar pattern of Pb and S was found throughout the  
559 sediment indicating this mineral was widely distributed. Fe did not show the same pattern and was not  
560 found to be partitioned with Pb. Mn was difficult to quantify through SEM/EDS, possibly due to lower  
561 total concentrations of this element in the sediment.

562 **3.4 Conceptual model for dissolved Pb mobilisation**

563 The results from the current study were used to create a simple conceptual model showing the key  
564 geochemical mechanisms controlling the release and attenuation of Pb. The model contrasts two key  
565 hydrological runs, the prolonged 3 wwet run with a short period of drainage and the constant flood  
566 (control) run. Both include a prolonged water residence time to allow reactions to occur at the  
567 sediment/water interface, however, the period of drainage for the 3 wwet run allows exposure to  
568 atmospheric conditions, particularly at the surface. These conditions would promote the oxidation of  
569 galena and result in the release of dissolved Pb into surface water upon re-wetting. In contrast, for the  
570 prolonged flood period with no period of drainage there would be little exposure to atmospheric  
571 conditions and oxygen, particularly deeper in the sediment. This would serve to reduce the rate of  
572 galena oxidation and conditions may 'stagnate'. High dissolved Pb concentrations and dissolution of  
573 sulphate bearing minerals such as gypsum may result in saturation with respect to anglesite leading  
574 to the attenuation of dissolved Pb. The 3wwet run is shown at the top of the mesocosm and the flood  
575 run at the bottom of mesocosm to highlight where the pattern of dissolved Pb mobilisation/ attenuation  
576 is most pronounced for each run. The dashed arrows indicate the depth at which key mechanisms  
577 have less of an influence on the pattern of dissolved Pb release.



Simple conceptual model summarising the key hydrogeochemical mechanisms controlling the release and attenuation of Pb in response to 'riverbank' inundation and drainage

578

579 Fig. 11. Simple conceptual model showing the key geochemical mechanisms controlling the release  
 580 and attenuation of Pb.

581 The environmental factors controlling diffuse pollution from contaminated riverbank sediment are  
 582 currently seen as a 'black box' from a process perspective. The current study is the first to uncover  
 583 the key mechanisms responsible for dissolved Pb release into the riverine environment.

584 Compared to a previous study of Zn mobilisation in riverbank sediments (Lynch et al 2017), the  
 585 current research has found that the geochemical mechanisms controlling the release of dissolved Pb  
 586 are dissimilar. Due to different geochemical mechanisms controlling mobilisation for Pb and Zn, the  
 587 patterns of release were found to be different in response to the flood/ drainage runs. High  
 588 concentrations of dissolved Zn were released (i) immediately on flood wetting following a long dry  
 589 antecedent period, and (ii) in response to prolonged flooding, at the bottom of the mesocosm, due to  
 590 reductive dissolution processes. In the current study, the highest concentration of dissolved Pb  
 591 release was observed at the surface, in response to longer/ more frequent flood periods, with  
 592 intermittent drainage episodes that promoted oxic conditions. 3.5 Environmental risk of contaminated  
 593 sediments

594 Pb is listed as a priority substance in the Water Framework Directive 2013/39/EU, 12th August 2013,  
 595 amending directives 2000/60/EC and 2008/105/EC in the field of water policy. These directives note

596 that maximum allowable concentrations (MAC) should be taken into account in the river basin  
 597 management plans covering period 2015 to 2021. For inland surface waters the annual average for Pb  
 598 and its compounds is 1.2 µg l<sup>-1</sup> (bioavailable). Where risk to, or via, the aquatic environment as a result  
 599 of acute exposure has been identified, maximum allowable concentrations (MAC = 14 µg l<sup>-1</sup>) have been  
 600 applied. The EU standard takes into the account the influence of DOC on the toxicity of Pb but unlike  
 601 the standard for Zn it does not require consideration of Ca. A metal bioavailability assessment tool has  
 602 been developed for Pb that takes into consideration the influence of DOC. Using the highest  
 603 concentrations of DOC 4.9 mg L<sup>-1</sup> measured in the current study the calculated predicted no effect  
 604 concentration (PNEC) of Pb (the calculated dissolved concentration of Pb that is equivalent to the  
 605 EQSavailable for local water conditions at the site) is 5.88 µg L<sup>-1</sup>.

606 Comparing the above standards to the results from dilution calculations (Table 7) it can be seen that  
 607 dissolved Pb concentrations for all runs exceed MAC and PNEC and therefore would be expected to  
 608 cause adverse environmental effects and pose a significant environmental risk.

609 Table 7.  
 610 Diluted Pb min and max average concentrations for 1st and 2nd mesocosm experiments

Mesocosm experiment #	Pb mg l <sup>-1</sup>	Pb after dilution µg l <sup>-1</sup>
1st experiment (max)	21.5	34.4
1st experiment (min)	10.8	17.28
2nd experiment (max)	10	16
2nd experiment (min)	3.8	6.08

611

612 There are currently no mandatory threshold values for trace metal contaminants in river sediments in  
 613 the UK and Europe. This is due to (i) The challenges of setting fixed standards in river systems where  
 614 contamination is spatially highly variable and (ii) limited toxicological data (Environment Agency,  
 615 2008). Catchments with a long history of mining are often naturally highly mineralised and difficulties  
 616 can arise when assessing the precise environmental risk contaminated soils and sediment may pose  
 617 (Dennis et al., 2003). There are however interim sediment quality guideline values developed by the  
 618 Environment Agency (Environment Agency, 2008) that are used to trigger further investigation.

619 Predicted effect level (PEL) is the level above which adverse biological effects are expected to occur.

620 It can be seen that sediment sampled for the 1<sup>st</sup> and 2<sup>nd</sup> mesocosm experiments contained high

621 concentrations of Pb (Table 5). All samples far exceed predicted effect level (PEL) concentrations and  
622 therefore could pose a significant environmental risk. It should be noted that these interim standards  
623 relate to in-channel sediments, rather than river bank sediments, but in the absence of other  
624 standards relating to sediment they have been used as a guide.

625 PEL values relate to total metals (including residual forms) and therefore provide no indication of the  
626 potential bioavailability of trace metal contaminants. A recent study of Pb contaminated soil found that  
627 LC 50 values (concentration of Pb causing 50% mortality) for earth worms were far lower for acidic  
628 soils, pH 4.96 (1161 mg Kg<sup>-1</sup>) compared to neutral, pH 6.94 (4648 mg Kg<sup>-1</sup>) or alkaline, pH 8.45 (7851  
629 mg Kg<sup>-1</sup>) soils and concluded that soil properties are important factors that modify bioavailability  
630 (Wijayawardena et al. 2017). In the current study the low inorganic carbon concentrations of the  
631 sediment indicate a slightly acidic environment that may favour increased bioavailability. Furthermore  
632 all concentrations of Pb measured in the current study exceeded all LC 50 values regardless of pH.  
633 The high concentration of Pb present in the most labile fractions of the sediment indicate that  
634 dissolved Pb could easily be released into pore and surface water in response to environmental  
635 perturbations with potentially serious adverse effects on water quality, aquatic flora and fauna and the  
636 surrounding agricultural and grazing land (Walling et al. 2003; Foulds et al. 2014).

#### 637 **4. Conclusions**

638 The Cwmystwyth mine has been identified as a top 30 priority mining 'impacted' waterbody in western  
639 Wales river basin district (Environment Agency 2012b). Although mining has ceased at the site the  
640 sediment remains severely Pb-contaminated. Results of the current study indicate the sediment is  
641 likely to act as source of dissolved Pb pollution to the Afon Ystwyth. Historical studies have found high  
642 concentrations of Pb (68 µg l<sup>-1</sup>) in the river water half a km below the Cwmystwyth mine area with  
643 concentrations remaining high (58 µg l<sup>-1</sup>) up to 7.5 km downstream although more recent studies  
644 found concentrations of dissolved Pb to be below detection (Montserrat 2010).

645 A previous mesocosm study by Lynch et al. (2017) found high concentrations of dissolved Zn may be  
646 released from stream riverbanks over prolonged flood periods due to the reductive dissolution of Mn  
647 (hydr)oxides. Pb is generally reported as less mobile than dissolved Zn. However, results from the  
648 current study indicate that high concentrations of dissolved Pb could be released in response to

649 longer or more frequent flood events where periodic drainage events serve to keep conditions more  
650 oxic, particularly at the surface.

651 This is a concern because climate projections indicate a rise in the occurrence of localized heavy  
652 rainfall events, particularly in winter (DEFRA 2012b). Projected increases in flood events, particularly  
653 during winter months could result in a rise in river stage leading to prolonged inundation of river bank  
654 sediment and the mobilisation of dissolved Pb. Anglesite solubility may control dissolved Pb  
655 concentrations with depth, but have little control at the sediment surface where continual oxidation of  
656 galena and subsequent releases of dissolved Pb may occur. Where flood conditions subside a fall in  
657 river stage and exfiltration could result in a pulse of dissolved Pb released into river systems. Dilution  
658 calculations indicate that concentrations of dissolved Pb released are likely to exceed MAC in river  
659 water and therefore pose a significant environmental risk.

660 This study is unique in linking key hydrological processes that may occur due to climate change to  
661 hydrogeochemical mechanisms controlling dissolved Pb mobilisation. The mineralogy at the  
662 Cwmystwyth site is common to many mining impacted sites and it is likely that the mechanisms  
663 identified in the current study would be widespread in the UK and worldwide. As these pollution  
664 events are transient the 'exact sources' of Pb pollution would be difficult to identify in the field in the  
665 absence of continuous sampling methodologies. As a result Pb pollution events could go unnoticed.  
666 The authors suggest that further field studies are carried out that focus on understanding how stream-  
667 floodplain connectivity could drive diffuse Pb pollution at mining impacted sites particularly under  
668 variable hydrometeorological conditions.

#### 669 **Acknowledgements**

670 This research was funded by NERC ID: NE/J500240/1

#### 671 **Conflicts of Interest**

672 The authors declare no conflict of interest



673 **5. References**

- 674 Appelo CAJ, Postma D. *Geochemistry, groundwater and pollution*. Leiden, The Netherlands: A.A.  
675 Balkema Publishers, 2010.
- 676 Astillerosa JM, Godelitsasb A, Rodríguez-Blancoc JD, Fernández-Díaza L, Prietod M, Lagoyannise A,  
677 et al. Interaction of gypsum with lead in aqueous solutions. *Appl. Geochem.* 2010; 25: 1008-1016.
- 678 Baba AA, Adekola FA, Fapojuwo DPT, Otokhina FO. Dissolution kinetics and solvent extraction of  
679 lead from anglesite ore. *Journal of the Chemical Society of Nigeria* 2011; 36: 157-164.
- 680 Bartlett RJ. Characterizing soil redox behaviour. In: Sparks DL, editor. *Soil Physical Chemistry*. CRC  
681 Press, Boca Raton, FL., 1999, pp. 371-397.
- 682 Bick DE. *The Old Metal Mines of Mid-Wales. Part 1 Cardiganshire - South of Devil's Bridge*. Newent,  
683 Glos.: The Pound House, 1976.
- 684 Bradley SB. Long-term Dispersal of Metals in Mineralised Catchment by Fluvial Processes. In: Foster  
685 IDL, Gurnell AM, Webb BW, editors. *Sediment and Water Quality in River Catchments* John Wiley &  
686 Sons Ltd, 1995, pp. 161-177.
- 687 British\_Geological\_Survey. *British Regional Geology: Wales*. Nottingham: British Geological Survey,  
688 2007.
- 689 Buckby T, Black S, Coleman ML, Hodson ME. Fe-sulphate-rich evaporative mineral precipitates from  
690 the Rio Tinto, southwest Spain. *Mineral. Mag.* 2003; 67: 263-278.
- 691 Buekers J, Amery F, Maes A, Smolders E. Long-term reactions of Ni, Zn and Cd with iron  
692 oxyhydroxides depend on crystallinity and structure and on metal concentrations. *Eur. J. Soil Sci.*  
693 2008; 59: 706-715.
- 694 Burton GA. Metal Bioavailability and Toxicity in Sediments. *Crit. Rev. Environ. Sci. Technol.* 2010; 40:  
695 852-907.
- 696 Burton ED, Phillips IR, Hawker DW. Geochemical Partitioning of Copper, Lead and Zinc in Benthic,  
697 Estuarine Sediment Profiles. *J. Environ. Qual.* 2005; 34: 263-273.
- 698 Byrne P, Reid I, Wood PJ. Stormflow hydrochemistry of a river draining an abandoned metal mine:  
699 the Afon Twymyn, central Wales. *Environ Monit Assess* 2013; 185: 2817–2832.
- 700 Byrne P, Wood PJ, Reid I. The impairment of river systems by metal mine contamination: A review  
701 including remediation options. *Critical Reviews in Environmental Science and Technology*. *Crit. Rev.*  
702 *Environ. Sci. Technol.* 2012; 42: 2017-2077.
- 703 Byrne P, Reid I, Wood PJ. Sediment geochemistry of streams draining abandoned lead/zinc mines in  
704 central Wales: the Afon Twymyn. *Journal of Soils and Sediments* 2010; 10: 683-697.

705 Caetano M, Madureira MJ, Vale C. Metal remobilisation during resuspension of anoxic contaminated  
706 sediment: short-term laboratory study. *Water, Air, and Soil Pollution* 2003; 143: 23-40.

707 Cama J, Acero P, Ayora C, Lobo A. Galena surface reactivity at acidic pH and 25°C based on flow-  
708 through and in situ AFM experiments. *Chemical Geology* 2005; 214: 309-330.

709 Carroll SA, O'Day PA, Piechowski M. Rock-water interactions controlling zinc, cadmium, and lead  
710 concentrations in surface waters and sediments, US Tri-State Mining District. 2. Geochemical  
711 interpretation. *Environ. Sci. Technol.* 1998; 32: 956-965.

712 Centre for Ecology and Hydrology. National river flow archive. 2015. Accessed: 101015. Available  
713 from: <http://www.ceh.ac.uk/data/nrfa/data/station.html?63004>

714 Charlatchka R, Cambier P. Influence of reducing conditions on solubility of trace metals in  
715 contaminated soils. *Water, Air, Soil Pollut.* 2000; 118: 143-167.

716 Chibuike GU, Obiora SC. Heavy metal polluted soils: Effect on plants and bioremediation methods.  
717 *Appl. and Env. Soil Sci.* 2014; 2014: 1-11.

718 Cid N, Ibanez C, Palanques A, Prat N. Patterns of metal bioaccumulation in two filter-feeding  
719 macroinvertebrates: exposure distribution, inter-species differences and variability across  
720 developmental stages. *Sci. Total Environ.* 2010; 408: 2795-806.

721 Ciszewski D and Grygar Tomas Matys. A review of flood-related storage and remobilisation of heavy  
722 metal pollutants in river systems. *Water, Air, & Soil Pollution* 2016, 227 – 239.

723 Collins A, Ohandja D, Hoare D, Voulvoulis N. Implementing the Water Framework Directive: a  
724 transition from established monitoring networks in England and Wales. *Environmental Science &*  
725 *Policy* 2012; 17: 49-61.

726 Cravotta CA. Dissolved metals and associated constituents in abandoned coal-mine discharges,  
727 Pennsylvania, USA. Part 2: Geochemical controls on constituent concentrations. *Appl. Geochem.*  
728 2008; 23: 203-226.

729 DEFRA. Climate Change Risk Assessment for the water sector. Project Code GA0204. In: DEFRA,  
730 editor. Crown, 2012a.

731 DEFRA. Climate Change Risk Assessment for the Floods and Coastal Erosion Sector Project code  
732 GA0204, Wallingford, 2012b.

733 Dennis IA, Macklin MG, Coulthard TJ, Brewer PA. The impact of the October-November 2000 floods  
734 on contaminant metal dispersal in the River Swale catchment, North Yorkshire, UK. *Hydrological*  
735 *Processes* 2003; 17: 1641-1657.

736 Du Laing G, Rinklebe J, Vandecasteele B, Meers E, Tack FMG. Trace metal behaviour in estuarine  
737 and riverine floodplain soils and sediments: A review. *Sci. Total Environ.* 2009; 407: 3972-3985.

738 Du Laing G, Vanthuyn DR, Vandecasteele B, Tack FM, Verloo MG. Influence of hydrological regime  
739 on pore water metal concentrations in a contaminated sediment-derived soil. *Environ. Pollut.* 2007;  
740 147: 615-625.

741 Dzombak DA, Morel FMM. Adsorption of inorganic pollutants in aquatic systems. *Journal of Hydraulic*  
742 *Engineering-Asce* 1987; 113: 430-475.

743 Environment\_Agency. Prioritisation of abandoned non-coal mine impacts on the environment.  
744 SC030136/R2 The national Picture Environment Agency, 2012a.

745 Environment\_Agency. Prioritisation of abandoned non-coal mine impacts on the environment.  
746 SC030136/R6 The Western Wales River Basin District., 2012b.

747 Environment\_Agency. Prioritisation of abandoned non-coal mine impacts on the environment project  
748 summary SC030136/S14. Environment Agency, 2010.

749 Environment\_Agency. Assessment of metal mining contaminated river sediments in England and  
750 Wales. Environment Agency, Bristol, 2008.

751 Evans D. Chemical and physical partitioning in contaminated stream sediments in the River Ystwyth,  
752 Mid-Wales. *Environmental Geochemistry and Health* 1991; 13: 84-92.

753 Fairchild IJ, Spotl C, Frisia S, Borsato A, Susini J, Wynn PM, et al. Petrology and geochemistry of  
754 annually laminated stalagmites from an Alpine cave (Obir, Austria): seasonal cave physiology.  
755 Geological Society, London, Special Publications 2010; 336: 295-321.

756 Farnsworth CE, Hering JG. Inorganic Geochemistry and Redox Dynamics in Bank Filtration Settings.  
757 *environmental science & technology* 2011; 45: 5079-5087.

758 Foulds SA, Brewer PA, Macklin MG, Haresign W, Bretson RE, Rassner SME. Flood-related  
759 contamination in catchments affected by historical metal mining: An unexpected and emerging hazard  
760 of climate change. *Sci. Total Environ.* 2014: 476-477.

761 Fuge R, Laidlaw IMS, Perkins WT, Rogers KP. The influence of acidic mine and spoil drainage on  
762 water quality in the mid-Wales area. *Environmental Geochemistry and Health* 1991; 13: 70-75.

763 Galan E, Gomex-Ariza JL, Gonzalez I, Gernandez-Caliani JC, Morales E, Giraldez I. Heavy metal  
764 partitioning in river sediments severely polluted by acid mine drainage in the Iberian Pyrite Belt.  
765 *Applied Geochemistry* 2003; 18: 409-421.

766 Gambrell., Delaune RD, Patrick JRW. Redox Processes in Soils following Oxygen Depletion. In:  
767 Jackson MB, Davies, D.D., Lambers, H., editor. *Plant Life Under Oxygen Deprivation*. SPB Academic  
768 Publishing, The Hague, 1991, pp. 101-117.

769 Gotoh S, Patrick WH. Transformation of iron in a waterlogged soil as influenced by redox potential  
770 and pH. *Soil Science Society of America Journal* 1974; 38: 66-71.

771 Grundl T, Delwiche J. Kinetics of Ferric Oxyhydroxide precipitation. *Journal of Contaminant Hydrology*  
772 1993; 14: 71-97.

773 Harris DL, Lottermoser BG, Duchesne J. Ephemeral acid mine drainage at the Montalbion silver mine,  
774 north Queensland. *Australian Journal of Earth Sciences* 2003; 50: 797 - 809.

775 Hudson-Edwards KA. Sources, mineralogy, chemistry and fate of heavy metal-bearing particles in  
776 mining-affected river systems. *Mineral. Mag.* 2003; 67: 205-217.

777 Hughes SJS. *The Cwmystwyth Mines*. Vol 17: Northern Mine Research Society, 1981.

778 Krause S, Hannah DM, Fleckenstein JH, Heppell CM, Kaeser D, Pickup R, et al. Inter-disciplinary  
779 perspectives on processes in the hyporheic zone. *Ecohydrology* 2010; 4: 481-499.

780 Kuechler R, Klause N, Zorn T. Investigation of gypsum dissolution under saturated and unsaturated  
781 water conditions. *Ecological Modelling* 2004; 176: 1-14.

782 Lee G, Bigham JM, Faure G. Removal of trace metals by coprecipitation with Fe, Al and Mn from  
783 natural waters contaminated with acid mine drainage in the Ducktown Mining District, Tennessee.  
784 *Appl. Geochem.* 2002; 17: 569-581.

785 Leinz RW, Sutley SJ, Desborough GA, Briggs PH. An Investigation of the Partitioning of Metals in  
786 Mine Wastes Using Sequential Extractions. ICARD 2000: Proceedings from the Fifth International  
787 Conference on Acid Rock Drainage 2. U.S. Geological Survey, Denver, Colorado, 2000.

788 Lesven L, Lourino-Cabana B, Billon G, Recourt P, Ouddane B, Mikkelsen O, et al. On metal  
789 diagenesis in contaminated sediments of the Deule river (northern France). *Appl. Geochem.* 2010; 25:  
790 1361-1373.

791 Linge KL. Methods for Investigating Trace Element Binding in Sediments. *Critical Reviews in*  
792 *Environmental Science & Technology* 2008; 38: 165-196.

793 Lovley DR, Phillips EJP. Manganese inhibition of microbial iron reduction in anaerobic sediments.  
794 *Geomicrobiology Journal* 1989; 6: 145-155.

795 Lovley DR, Phillips EJP. Competitive Mechanisms for Inhibition of Sulfate Reduction and Methane  
796 Production in the Zone of Ferric Iron Reduction in Sediments. *Appl. Environ. Microb.* 1987; 53: 2636-  
797 2641.

798 Lovley DR, Phillips EJP. Availability of Ferric Iron for Microbial Reduction in Bottom Sediments of the  
799 Freshwater Tidal Potomac River. *Appl Environ Microb.* 1986; 52: 751-757.

800 Lynch SFL, Batty LC, Byrne P. Critical control of flooding and draining sequences on the  
801 environmental risk of Zn-contaminated riverbank sediments. *J. Soils Sediments* 2017; 17: 2691-2707.

802 Lynch SFL, Batty LC, Byrne P. Environmental risk of metal mining contaminated river bank sediment  
803 at redox-transitional zones. *Minerals* 2014; 4: 52-73.

804 Mayes WM, Potter HAB, Jarvis AP. Riverine Flux of Metals from Historically Mined Orefields in  
805 England and Wales. *Water, Air, Soil Pollut.* 2013; 224: 1425.

806 Merrington G, Alloway BJ. The transfer and fate of Cd, Cu, Pb, and Zn from two historic metalliferous  
807 mine sites in the U.K. *Appl. Geochem.* 1994; 9: 677-687.

808 MET Office. Climate. Met Office. 2016. Accessed: 170816. Available from:  
809 <http://www.metoffice.gov.uk/public/weather/climate/gcm3c7x2r>.

810 Met Office (2017): UKCP09: Met Office regional land surface climate observations - long term  
811 averages for administrative regions and river basins. Centre for Environmental Data Analysis.  
812 Accessed: 050418. Available from:  
813 <http://catalogue.ceda.ac.uk/uuid/51132aea5ed0433ca338d32a912e3976>

814 Montserrat AM. Environmental impact of mine drainage and its treatment on aquatic communities.  
815 Water Sciences Group. PhD. University of Birmingham, 2010.

816 Macklin MG, Dowsett RB. The Chemical and Physical Speciation of Trace-Metals in fine-grained  
817 overbank flood sediments in the Tyne basin, Northeast England. *Catena* 1989; 16: 135-151.

818 Natural Resources Wales. A Metal Mines Strategy for Wales. Natural Resources Wales, Wales, 2004.

819 Neal C, Reynolds B, Neal M, Pugh B, Hill L, Wickham H. Long-term changes in the water quality of  
820 rainfall, cloud water and stream water for moorland, forested and clear-felled catchments at  
821 Plynlimon, mid-Wales. *Hydrology and Earth System Sciences* 2001; 5: 459-476.

822 Nordstrom DK, Alpers CN. Geochemistry of Acid Mine Waters. In: Plumlee GSaL, M.J., editor. *The*  
823 *Environmental Geochemistry of Mineral Deposits. Part A: Processes, Techniques, and Health Issues.*  
824 6A. Society of Economic Geologists, Inc. , Colorado, USA, 1999, pp. 133-160.

825 Oxford Instruments. INCAEnergy Applications training notes. Bucks: Oxford Instruments, 2008.

826 Palumbo-Roe B, Wragg J, Cave M, Wagner D. Effect of weathering product assemblages on Pb  
827 bioaccessibility in mine waste: implications for risk management. *Environmental Science & Pollution*  
828 *Research* 2013; 20: 7699 - 7710.

829 Palumbo-Roe B, Wragg J, Banks VJ. Lead mobilisation in the hyporheic zone and river bank  
830 sediments of a contaminated stream: contribution to diffuse pollution. *J. Soils Sediments* 2012; 12:  
831 1633-1640.

832 Poulton SW, Canfield DE. Development of a sequential extraction procedure for iron: implications for  
833 iron partitioning in continentally derived particulates. *Chem. Geol.* 2005; 214: 209-221.

834 Ross S. Soil Processes. New York: Routledge, 1989.

835 Shaheen SM, Rinklebe J, Rupp H, Meissner R. Temporal dynamics of pore water concentrations of  
836 Cd, Co, Cu, Ni, and Zn and their controlling factors in a contaminated floodplain soil assessed by  
837 undisturbed groundwater lysimeters. *Environ Pol* 2014; 191: 223-231.

838 Sharma P, Dubey RS. Lead toxicity in plants. *Braz. J. Plant Physiol* 2005; 17: 35-52.

839 Shimadzu Scientific Instruments. List of Shimadzu Application Notes, 2014.

840 Smith K. Metal sorption on mineral surfaces: an overview with examples relating to mineral deposits  
841 vol 6A. The environmental geochemistry of mineral deposits part a: processes, techniques and health  
842 issues. Society of Economic Geologists, Colorado, USA, 1999.

843 Stumm W, Sulzberger B. The Cycling of Iron in Natural Environments: considerations based on  
844 laboratory studies of heterogeneous redox processes. *Geochimica Et Cosmochimica Acta* 1992; 56:  
845 3233-3257.

846 Tessier A, Campbell PGC, Bisson M. Sequential Extraction Procedure for the speciation of particulate  
847 trace metals. *Analytical Chemistry* 1979; 51: 844-851.

848 Torres E, Ayora C, Canovas CR, Garcia-Robledo E, Galvan L, Sarmiento AM. Metal cycling during  
849 sediment early diagenesis in a water reservoir affected by acid mine drainage. *Sci. Total Environ.*  
850 2013; 461-462: 416-429.

851 Tripole S, Gonzalez P, Vallania A, Garbagnati M, Mallea M. Evaluation of the impact of acid mine  
852 drainage on the chemistry and the macrobenthos in the Carolina Stream (San Luis-Argentina).  
853 *Environ. Monit. Assess.* 2006; 114: 377-389.

854 Ullrich SM., Ramsey MH. Helios-Rybicka E. Total and exchangeable concentrations of heavy metals  
855 in soils near Bytom, an area of Pb/ Zn mining and smelting in Upper Silesia, Poland, *Applied*  
856 *Geochemistry* 1999; 14: 187-196.

857 US EPA. Standard operating procedure for GLNPO total alkalinity titration. . US EPA. Chicago 1992.

858 USGS. Lead-Rich Sediments, Coeur d'Alene River Valley, Idaho: Area, Volume, Tonnage and Lead  
859 Content, 2001.

860 vanLoon GW, Duffy SJ. *Environmental Chemistry*. Oxford, UK: Oxford University Press, 2011.

861 Walling DE, Owens PN, Carter J, Leeks GJL, Lewis S, Meharg AA, et al. Storage of sediment-  
862 associated nutrients and contaminants in river channel and floodplain systems. *Appl. Geochem.* 2003;  
863 18: 195-220.

864 Wang L, Yu R, Hu G, Tu X. Speciation and assessment of heavy metals in surface sediments of  
865 JinJiang River Tidal Reach, Southeast of China. *Environ. Monit. Assess.* 2010; 165: 491-499.

866 Wijayawardena MAA, Megharaj M, Naidu R. Bioaccumulation and toxicity of lead, influenced by  
867 edaphic factors: using earthworms to study the effect of Pb on ecological health. *J. Soils Sediments*  
868 2017; 17: 1064-1072.

869 Wilson B, Pyatt FB. Heavy metal dispersion, persistence, and bioaccumulation around an ancient  
870 copper mine situated in Anglesey, UK. *Ecotoxicology and environmental safety* 2007; 66: 224-231.

871 Wragg J, Palumbo-Roe B. Contaminant mobility as a result of sediment inundation: Literature review  
872 and laboratory scale pilot study on mining contaminated sediments. British Geological Survey Open  
873 Report, 2011, pp. 101.

874 Younger PL. Coalfield Abandonment: Geochemical processes and hydrochemical products. In:  
875 Nicholson K, editor. *Energy and the Environment: Geochemistry of fossil, nuclear and renewable*  
876 *resources* MacGregor Science, 1998, pp. 1-29.

877 Zakir HM, Shikazono N. Environmental Mobility and Geochemical Partitioning of Fe, Mn, Co, Ni, and  
878 Mo in sediments of an Urban River. *J. Environ. Chem. Ecotoxicol.* 2011; 3: 116-126.

879 Zadnik T. Monitoring of lead in topsoil, forage, blood, liver and kidneys in cows in a lead polluted area  
880 in Slovenia (1975-2002) and a case of lead poisoning (1993). *International Journal of Chemical*  
881 *Engineering* 2010; 2010: 1-6.

882 Zhang X, Yang L, Li Y, Li H, Wang W, Ye B. Impacts of lead/zinc mining and smelting on the  
883 environment and human health in China. *Environ Monit Assess* 2012; 184: 2261-2273.